CONSTRUCTION AND CHARACTERISTICS OF BF_3 TUBES USED IN DETERMINATION OF REACTOR PARAMETERS

by

MOHAMMED NASIM

B. Sc., Karachi University, 1952
M. Sc., Government College, Punjab University, 1954

A THESIS

submitted in partial fulfillment of the

requirements for the degree

MASTER OF SCIENCE

Department of Nuclear Engineering

KANSAS STATE UNIVERSITY
Manhattan, Kansas

1961

TABLE OF CONTENTS

INTRODUCTION

In the last two decades, a tremendous amount of work has been done to improve methods of neutron detection. The behavior of neutrons in matter is quite different from that of either charged particles or gamma rays. Since the neutrons are uncharged, no Coulomb forces come into play with either the orbital electrons or the nuclei. Thus for neutrons to affect matter, they must either enter the nucleus or come sufficiently close to it for the nuclear forces to act. There are several known mechanisms by which the interaction of neutrons with matter takes place and each of these processes is the basis of a potential method of detection. For example, in the neutrons-induced transmutations (n, α), (n, p), and (n, fission) reactions, the product particles make possible the detection, while in transmutations which result in radioactive product nuclei the subsequent decay of the radioactive nuclei gives information on the neutron flux which induces radioactivity.

Among the most extensively used methods is the B^{10} (n, α) reaction. Many factors make it highly satisfactory for this purpose, namely, the high cross section of the reaction and the simple energy dependence over a wide range of values. The reaction is easy to detect even in the presence of comparatively large gamma fluxes because of the high specific ionization and the large energy of the charged particles which are released. Solid boron as well as gaseous compounds can be used. Boron trifluoride (BF_3), being a comparatively stable compound, is used

frequently. Proportional counters filled with BF_3 gas have played an important part in the development of nuclear technology. They have been widely applied in the detection of thermal and epithermal neutrons in a variety of forms that range from multiple arrays of large counters providing high efficiency detection, for example, in time of flight spectrometers, to small counters which permit determination of flux distribution in reactor core assemblies.

The purpose of this investigation was as follows:

1. To get a better understanding of the different problems encountered in the construction and preparation of boron trifluoride counters.

2. To prepare the best BF_3 counter possible by using an inexpensive vacuum system.

3. To study the characteristics of the BF_3 counter obtained.

4. To use the prepared counters to determine certain subcritical reactor parameters.

PREPARATION OF THE COUNTERS

Construction of the Vacuum System

Since the production and purification of boron trifluoride gas had to be done under vacuum, a special design of vacuum system was necessary. The vacuum system had essentially to perform two functions:

1. Evacuate the whole system, including the counters.

2. Purify the gas under vacuum.

The photographs of the vacuum system are shown in Figs. 1 and 2. A Duco-seal pump, B, with an exhaust vent, I, was used to pump the pressure down to five microns. Mechanical vacuum pumps remove gases from the system by compressing them into a smaller volume, thus increasing their pressure until they force an oil-sealed valve open and then escape into the atmosphere. This compression works very well with the permanent gases such as air and hydrogen, but condensable vapors like water vapor and solvent vapors may cause a great deal of trouble. These vapors raise the vapor pressure of the oil, and thus limit the vacuum attainable by the pumps. The problem of obtaining high vacuum in presence of the condensable gases was solved by introducing an exhaust vent in the pump. A valving arrangement is provided which permits atmospheric air to enter the exhaust cycle of the pump. Because of the addition of this extra volume of air, the vapors coming from the system can be compressed only slightly to force the exhaust vent in. Thus since the vapors are not compressed to the critical point, they do not condense but pass instead in vapor form out of the pump. Even if some condensable material, such as water, should get into the oil in liquid form, the vented exhaust will clear the oil in a matter of seconds. This exhaust vent has proven to be effective even in the presence of BF_3 gas.

A Consolidated Electrodynamics glass oil diffusion pump, A, Fig. 1, was used to reduce the pressure to the range 10^{-5} to 10^{-6}

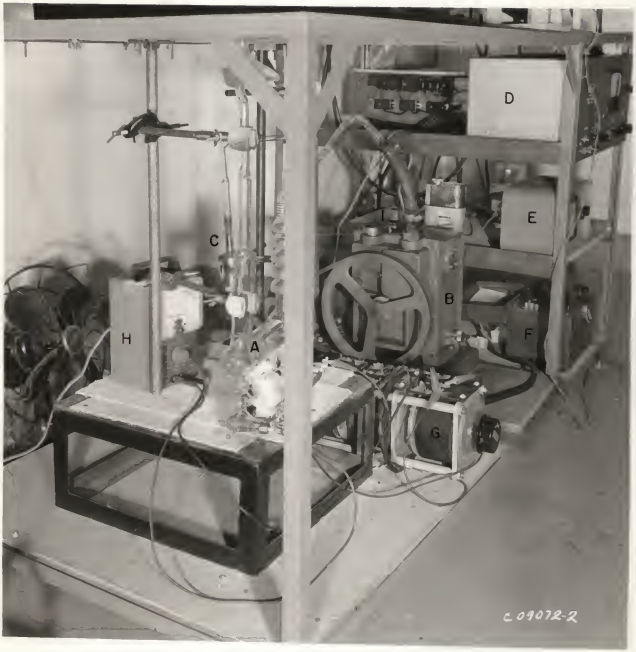

Fig. 1. Photograph of vacuum pumps and associated control panels for the ionization and Pirani gauges. A, diffusion pump; B, mechanical pump; C, Pirani gauge; D, control panel RG-21; E, control panel for GP-110 (Pirani gauge); F, potentiometer; G, variac; H, VTVM Heathkit; I, exhaust vent.

mm Hg. It consisted of three independent boilers, each containing a heater immersed directly in the operating liquid.

This pump was mounted on adjustable clamps and connected to the system. The whole system was then tested by a high-frequency Tesla coil. When all the leaks were sealed, the diffusion pump was filled with Dow Corning diffusion pump oil type 703 to approximately five mm above the heaters. After obtaining the backing pressure from the mechanical pump, the heaters were connected to the a-c mains through a variac transformer, G. Prolonged degassing of the oil was necessary to obtain the lowest pressure. In general, twelve to fourteen hours were necessary to obtain pressure of the order of 10^{-5} mm Hg. The right voltage for the heater was selected by operating the diffusion pump at different voltages and checking the pressure in the system with the ionization gauge control, D. The lowest pressure, 5×10^{-6} mm Hg, was obtained at 70 volts. This was then selected as the operating voltage. A general precaution is to avoid putting the diffusion pump to work before the pressure is reduced down to 10 microns. For this reason a Pirani gauge, C, type GP-110, obtained from Electrodynamics Corporation, was installed between the mechanical pump, B, and the oil diffusion pump, A. Pressure in the range of 0 to 2000 microns could be measured by this gauge.

For measuring pressures below one micron, Veco ion gauge type RG-75 together with a control panel, D, type RG-21, was used. The gauge contains a thoria-coated indium filament which does not oxidize if the filament accidentally comes in contact with air. The RG-75 was connected directly to the manifold, F,

as shown in Fig. 2. In a later design, the position of the gauge was changed as seen in Fig. 9, because it was found that a thin white film settled on its walls and changed its characteristics. Heating the tube walls to about 250° C helped in removing that film. The tube grid had to be outgassed at a pressure less than 10^{-4} mm Hg, because outgassing at higher pressures tends to blacken the walls due to sputtering of the tungsten in the grid.

Two Alpert valves V_1 and V_2, Fig. 2, were used to substitute for stopcocks between the pumps and the manifold and to disconnect the counters from the rest of the system. This type of vacuum valve was developed at the Westinghouse Laboratories. It essentially consists of a separate valve assembly which becomes a part of the vacuum system, and a driving mechanism which opens and closes the valve. Aside from the vacuum leads, the valve assembly contains only three mechanical parts: A copper cup, 1.75-inch diameter, a flexible Kovar diaphragm which allows a movement (up and down) of about 0.1 inch, and a Kovar nose, with a highly polished 45-degree conical surface, seated in the copper cup.

All of the joints in this valve were brazed (eutectic silver-copper soldered) simultaneously in a hydrogen furnace without the use of flux. The driving mechanism consisted of an outside screw and housing (stainless steel), a simple screw (silicon bronze), and a drive screw (stainless steel) which was bolted to the valve nose before the rest of the driver was installed. The external portion of the nose was machined to form a flat disk one inch in diameter. The simple screw (32 threads per inch)

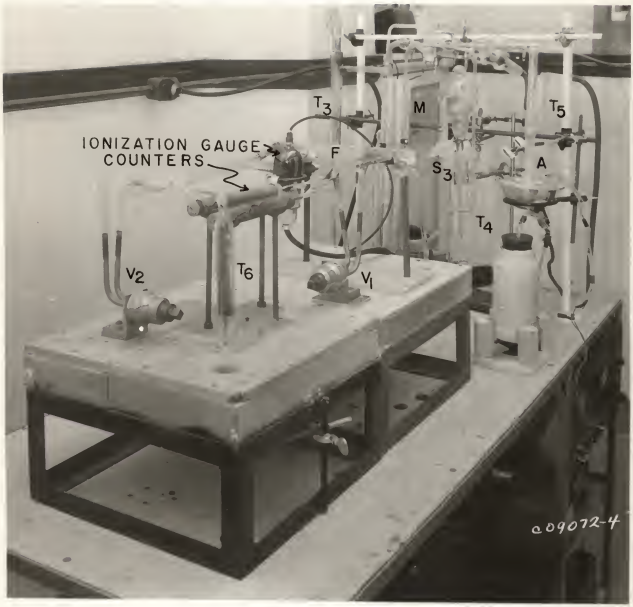

Fig. 2. Photograph of the filling system. A, 50-ml flask; T_3, T_4, T_5, T_6, traps; V_1, V_2, Alpert valves; M, manometer; F, manifold.

exerts its thrust against this flat disk which forms the thrust bearing. During the bake-out periods, the driving mechanism was removed completely.

A trap, T_6, Fig. 2, similar to the one used by Alpert (2), was placed between the high vacuum side and the diffusion pump to prevent the backstreaming of oil vapor in the high vacuum side of the system. The trap consisted of a standard reentrant glass trap into which corrugated copper was inserted so that the trap contained a large number of fine copper straws. This type of trap was designed originally to solve the usual problem encountered with a refrigerated reentrant trap, that is, as the liquid refrigerant evaporates, the cold level drops and the gas that had previously been absorbed is reevaporated into the system. In this design, it was intended to utilize the high thermal conductivity of the metallic insert so that the entire trap surface may remain cold despite large fluctuations in the liquid level. The trap also affords an extremely high ratio of length to diameter without greatly sacrificing the speed of the system. It was found later on, (3), that the trap worked efficiently even when the liquid level dropped to zero. Since then, such traps have been used in the nonreentrant portions of vacuum systems without refrigerants.

A mercury manometer, M, was used to measure the BF_3 gas pressure in the system during the process of filling the counters. A layer of 703 Dow Corning oil was placed on top of the mercury in order to avoid the Hg pressure which amounts to 1.3×10^{-4} mm at room temperature. About four to six hours were necessary to

pump down all the entrapped gases from the oil. Long contact of BF_3 gas with the oil seemed not to affect it to any appreciable extent.

A water pump was connected to the system by high vacuum rubber tubing through a phosphorous pentoxide trap to remove the BF_3 gas from the system when needed.

As the work proceeded, the BF_3 gas was found to react severely with the stopcock grease introducing impurities in the gas and spoiling the counter characteristics. It was decided to modify the system by cutting down the number of glass stopcocks to one. The modified system is illustrated in Fig. 9.

A Cu-Constantan thermocouple was also placed inside trap T_3. This thermocouple was used to measure the temperature of the gas evolved. The Cu-Constantan wires were sealed through an Electric Industries strain-free seal type D-60 TT-SX, which was soft soldered to the Kovar glass seal, as shown in Fig. 9. The glass side of this seal was connected to trap 3. The end of the thermocouple was placed about one inch above the bottom of the trap. A precision potentiometer type K_3, Leeds and Northrup, was used to measure the potential difference across the wires. Temperatures were determined by referring to the appropriate calibrated charts.

Construction of the Counters

Two fundamental principles should be considered in the construction of the counters:

1. The construction and preparation should be such as to permit the mechanism of the counter discharge to operate with a minimum of disturbing effects from unwanted agencies.

2. The construction procedure should insure that the desired conditions remain as permanently as possible.

The first principle requires that the counter cylinder should be made of a substance with high work function, and alkali metals should be especially avoided. This is important because the supply of secondary electrons, which causes the discharge to continue and thus defeat the processes quenching the discharge, is dependent on the work function. The number of secondary electrons can be greatly reduced by proper choice of cathode surface, and the counter will accordingly have better operating characteristics.

The second principle requires cleaning the counter thoroughly before sealing to the vacuum system. Any absorbed film of material will change the chemical composition of the gas in the counter, thus changing the properties of the counter accordingly. This is especially true with the counters filled with boron trifluoride gas.

Copper has been found to be a good material for the counter cylinders. Brass could also be used and is frequently available in suitable shapes. Both these materials were used in this investigation and the counters built are illustrated in Figs. 3 and 4.

The outer shell of counter (A), which served also as the cathode, was made of a seamless brass tube seven inches long, one

inch outside diameter, with a wall thickness of 0.03 inch. The anode, 1, was a 3-mil diameter tungsten wire. Tungsten was selected because it could be readily sealed to glass and heated successfully while the counter was being pumped. A piece of uniform, smooth, and clean tungsten wire was selected to avoid the local ionization which produces spurious counts, and to avoid the spread in gas multiplication and the spread in pulse height caused by the small eccentricities in the wire (21). The end of the anode wire, 1, was spotwelded at point 2, to the anode lead 3, which was sealed to glass at point 4. Point 2, where the wire was welded to the supports, was shielded with a glass sleeve, 5, in order to avoid the high local fields.

Details of the end cap, 6, are shown in Fig. 3(B). It was made of a solid piece of copper cylinder one inch in diameter and 5/8 inch long through which a cylindrical hole 1/2 inch in diameter and 9/16 inch long was drilled. A 1/2-inch diameter quartz tube, 7, 5/8 inch long, with a closed end, was placed in the drilled hole. A small hole was blown in the closed end by a fine oxygen-hydrogen flame before the quartz tube was placed in the drilled cylindrical hole. The anode wire, 1, was introduced through the hole, through the Nichrome spring, 8, and through a 7/16-inch diameter molybdenum disk, 9, in which a fine hole had been drilled. Pressure was applied on this disk and a small bead of pyrex glass, 10, was sealed to the wire to keep it under tension. A 1/4-inch copper disk, 11, was silver soldered as shown in Fig. 3(B) to close the end. A glass-copper seal, 12, Fig. 3 (A), was used as an insulator for the high-voltage electrode and

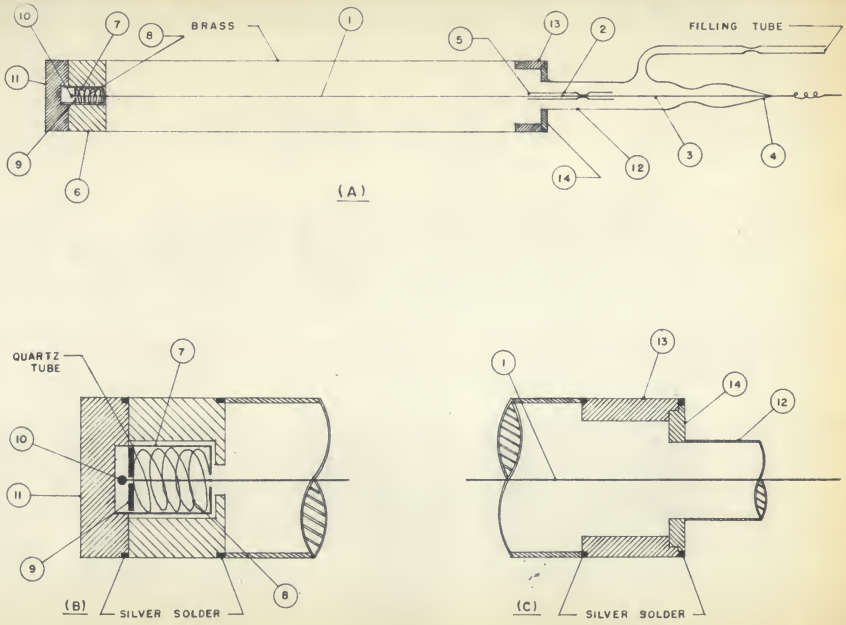

Fig. 3. Counter (A) including details of the end cap and the glass-to-metal seal.

also for connecting the counters to the vacuum system. Cylinder 13 is a piece of brass tubing one inch in diameter and 1/8 inch thick which was silver-soldered to the outer shell of the counter. A copper disk, 14, 3/32 inch thick, in which a 5/16-inch hole was drilled, was seated in the cylinder, 13, and silver-soldered to it. A glass-copper seal, 12, was fitted by force into this hole and was silver-soldered to the disk, 14. Details of this part of the counter are shown in Fig. 3(C).

Counter (B), Fig. 4, was constructed from a special 1-inch diameter glass-copper seal, 1, obtained from Larson Electronics Corporation, California. The copper part of this seal was 7 inches long. The end cap, 6, was the same as the one used in counter (A). This counter was easier in construction and proved to be better in quality, and was therefore preferred in most of the work.

Before connecting the counters to the vacuum system, they were cleaned with dilute nitric acid, washed thoroughly with distilled water, and dried in an oven at 200° C, thus removing most of the absorbed impurities. After connecting the counters to the vacuum system they were outgassed at 250° C for 12 hours and then at 400° C for two more hours. The pressure during the bake-out period was kept below 10^{-4} mm Hg. Baking out of the counter envelopes proved to have a great influence on the counter behavior later on.

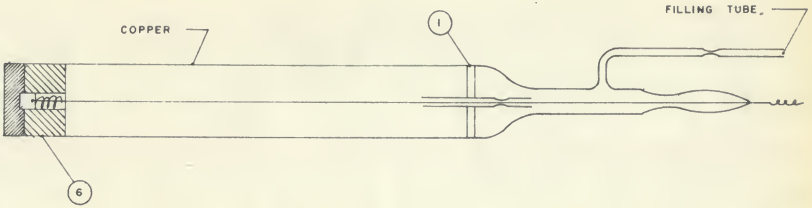

Fig. 4. Counter (B).

Effect of Impurities in the Boron Trifluoride Gas on the Counter Performance

On account of the unsatisfactory behavior of commercial boron trifluoride gas as a direct filling for pulse counters of high sensitivity, some preliminary work was carried out at the Chalk River Laboratories, in Canada, on the purification of boron trifluoride. It was found that the impurities most likely to interfere with the performance of boron trifluoride counters are oxygen, halogens, ammonia, water, nitrous and nitric oxides, sulphur dioxide, hydrogen fluoride and chloride, silicon tetrafluoride, and mercury vapors. Their influence has been attributed to electron capture and, in some cases, to dissociation of the molecules (22).

The electron attachment probability, h, for some of the gases mentioned above are presented in Table 1, (16). It is defined as the probability that an electron will attach to the molecule with which it collides. An electron will make, on the average, around 10^5 collisions in crossing a counter, the mean free path depending on the pressure. Considering this, the probability that the electron should attach to a neutral molecule should be less than 10^{-5}. Reported values for h are low for argon, carbon monoxide, hydrogen, nitrogen, and ammonia (16).

Table 1. Electron attachment probability, h (16).

Gas	h	Gas	h
CO	6.25×10^{-7}	H_2O	0.25×10^{-5}
NH_3	1.01×10^{-6}	$c\ell_2$	0.5×10^{-3}
C_2H_6	4.0×10^{-5}	SiF_4	1.48×10^{-5}
N_2O	1.63×10^{-4}	SO_2	10^{-4}
Air	0.5×10^{-5}	SF_6	0.936
O_2	0.25×10^{-3}		

h - probability that an electron will attach to the molecule with which it collides.

The h for air is 0.5×10^{-5}, which is close to the critical value of 10^{-5}, mentioned above. The figures for oxygen, water, and chlorine are all greater than this critical value, and therefore must be avoided.

Boron trifluoride generated inside a glass vacuum system usually contains silicon tetrafluoride (6, 14), an electronegative gas with attachment probability of 1.485×10^{-5}. Sulphur dioxide (7) and sulphur hexafluoride (13) have also been found in BF_3. Both are highly electronegative gases with attachment probabilities of 10^{-4} and 0.936, respectively.

The effects which silicon tetrafluoride, sulphur dioxide, and sulphur hexafluoride have on the plateau and the pulse size distribution of a proportional counter were investigated by Aponte and Korff (4). They obtained the attachment cross sections for these gases as follows:

The number of electrons at a distance dr is expressed as

$$dn = (\alpha - \eta)\, ndr$$

where α is the first Townsend coefficient, and η is the number of attachments per cm advanced in the direction of the field. Integrating, the number of electrons at a distance r can be written as

$$n = n_0 \exp \int (\alpha - \eta)\, dr \qquad (2)$$

The number of attachments per cm advanced can be written as

$$= (\bar{c}/\lambda)(1/v)(p/P)h \qquad (3)$$

where $\bar{c}$ is the average agitational velocity of the electron, λ is its collision mean free path, $(\bar{c}/\lambda)$ is the frequency of the collision, and v is the drift velocity along the field of the counter, making (1/v) the time needed to cover one cm along the field. Therefore $(\bar{c}/\lambda)(1/v)$ is the number of collisions the electrons make while covering a distance of one cm along the field. Since only a fraction of these collisions are with the electronegative molecules, the number of collisions with the impurity can be obtained by multiplying the above expression by (p/P), the ratio of the pressure of the electronegative gas to that of BF_3. Multiplying $(\bar{c}/\lambda)(1/v)(p/P)$ by h gives the number of attachments per cm along the path of the electron.

From equation (3), it can be seen that η is a function of p, and since α is a constant for the counter, by increasing the pressure of the electronegative gas, fewer electrons will reach the wire. This will cause a variation in the pulse size distribution of the counter, with the consequent loss of the counting rate when the pulse becomes smaller than the discrimination level of the amplifier. This will affect the plateau of the counter.

Since $(\bar{c}/\lambda)(1/v) = N_o$, where N_o is the total number of collisions the electron makes in going from cathode to point r, then equation (3) can be written as

$$n = n_o \exp\left[\int \alpha dr - h N_o (p/P) r\right] \qquad (4)$$

where h was assumed as a constant of the electronegative gas.

If the collision cross section is given by

$$\sigma_c = 1/\lambda \; n \qquad (5)$$

where λ is the mean free path for collision of the electrons in the electronegative gas, and N is the number of electronegative molecules per cm^3, then the attachment cross section is given by

$$\sigma_a = \sigma_c \, h = h/\lambda N \qquad (6)$$

The effect of silicon tetrafluoride, sulphur hexafluoride, and sulphur dioxide on the counter plateau is shown in Figs. 5, 6, and 7, respectively (4). From Fig. 5, it is seen that a very small amount of silicon tetrafluoride is needed to damage a counter. An amount of silicon tetrafluoride equal to 0.2 per cent reduces the length of plateau by 50 volts. The attachment cross section for this gas obtained by Aponte and Korff (4) was 5.12×10^{-20} cm^2. The strong effect of sulphur hexafluoride is due to its large attachment probability. The attachment cross section was found (4) to be 4.26×10^{-15} cm^2.

Sulphur dioxide also has a high attachment probability of 10^{-4}. The amount of this gas permitted, without the counter being affected beyond the limits of tolerance, is given as 0.01 per cent (4).

No direct measurements as to the effects of these impurities

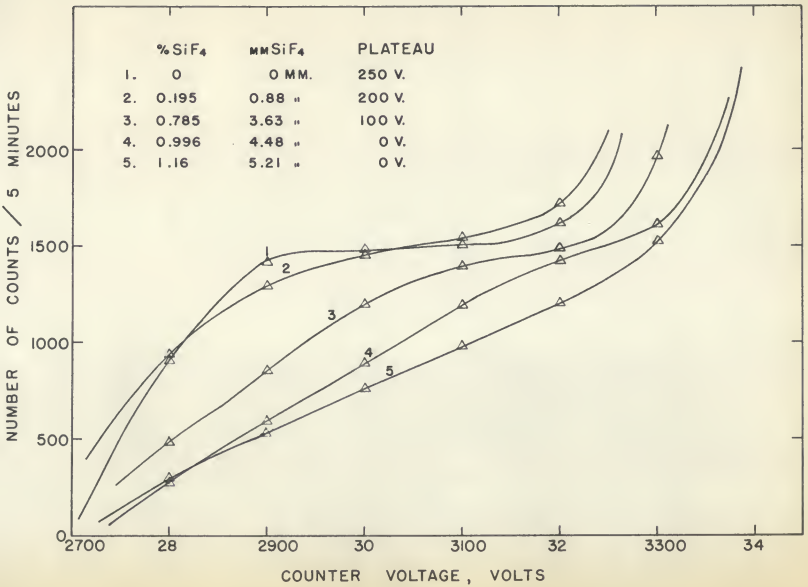

Fig. 5. Effect of SiF_4 on the plateau of a counter with 45 cm pressure of BF_3.

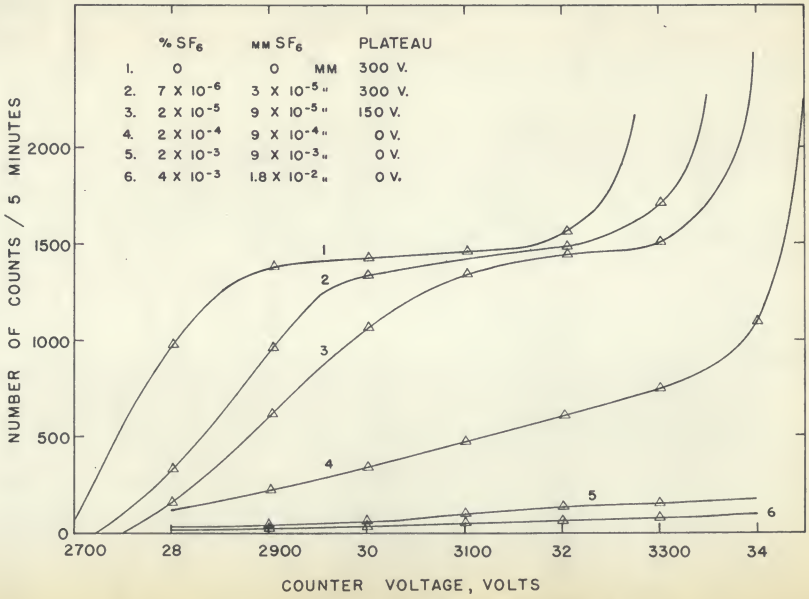

Fig. 6. Effect of SF_6 on the plateau of a counter with 45 cm pressure of BF_3.

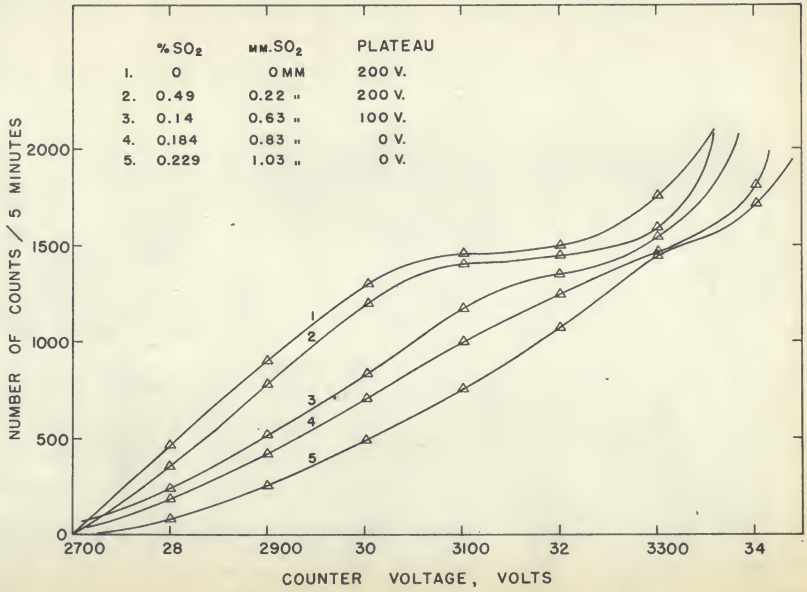

Fig. 7. Effect of SO_2 on the plateau of a counter with 45 cm pressure of BF_3.

on the counter performance were conducted during this investigation, although various precautions necessary to avoid these impurities were taken in order to get a counter with good characteristics. Stopcock greases containing silicon or sulphur were specifically avoided.

Preparation of Boron Trifluoride Gas

The nominal composition of commercial boron trifluoride is 20 atom per cent B^{10} and 80 atom per cent B^{11}. The reaction B (n, α) occurs only for the B^{10} isotope. The B^{11} component performs no useful function. An extensive amount of work on the preparation of pure boron trifluoride gas from commercial cylinder gas was undertaken at A.E.R.E., Harwell, by Hudswell, Nairn, and Wilkinson (14). Various precautions were necessary as boron trifluoride gas reacts very readily with the stopcock grease and the silica in the glass. All the stopcocks were replaced by mercury cut-off valves and the glass container used for storing BF_3 by stainless steel in order to avoid any prolonged contact with the glass, and polytetrafluoroethylene was chosen as the gasket material for this vessel. They reported that rough fractionation of the cylinder gas by repeated condensation at -120° C and prolonged pumping of the permanent gases from solid boron trifluoride were not effective in improving the gas characteristics. Hence they proceeded via the additives with diethyl ether and prepared boron trifluoride diethyl ether complex by passing dried boron trifluoride gas through a flask filled with analytically

pure ether. The product was fractionally distilled in an efficient column packed with glass helics and the fraction boiling at 126° C was collected. They recommended fractionation under vacuum in order that the product could be stored for a longer period of time. Their next step was the preparation of the BF_3CaF_2 complex.

They dried CaF_2 in vacuum at 300° C and added boron trifluoride etherate to the flask. The etherate reacts with calcium fluoride at temperatures below 100° C to form CaF_2BF_3 with the liberation of ether. They recommended dry steel containers for the storage of this complex. The replacement of the diethyl ether boron trifluoride complex by the dimethyl ether complex was recommended by Lloyd, Hodges, and Weinstock (17) because of its higher volatility.

Air-free boron trifluoride gas was prepared from the BF_3CaF_2 complex by Bistiline (5) and later on by Fowler and Tuncliffe (10). Their method was adopted in this investigation with minor changes. The detailed method used was as follows.

A known amount of 96 per cent enriched CaF_2BF_3 complex, obtained from Oak Ridge National Laboratory, was kept in the 50-ml round bottom flask A, Fig. 8. After outgassing the counters as described in the section on construction of the counters, the system was pumped down to less than 10^{-5} mm Hg. The Alpert valve V_1 was closed, a heating mantle was placed around flask A, and the complex was heated to 100° C for two hours, or until the pressure was reduced to 10^{-5} mm Hg, indicating the removal of any moisture. Traps T_2 and T_3 were surrounded by Dewar flasks

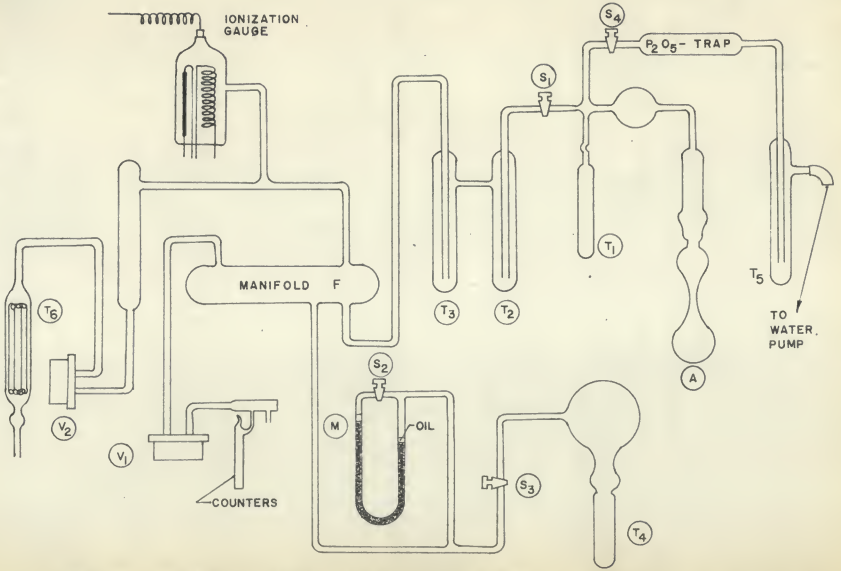

Fig. 8. Schematic diagram of the filling system. A, flask; T_1, T_2, T_3, T_4, T_5 traps; V_1, V_2 Alpert valves; S_1, S_2, S_3, S_4 glass stopcock; T_6 copper trap; M, manometer; F, manifold.

filled with solid CO_2 - acetone mixture and liquid air, respectively.

The complex was heated to 150° C and the pumping was continued until the pressure was less than 10^{-5} mm Hg. Stopcock S_1 was closed and the temperature of the compound was raised to between 180° and 200° C. The gas started to evolve. As indicated by Hudswell, Nairn, and Wilkinson (14), the gas evolved during the first ten minutes included most of the volatile impurities. For this reason trap T_1 was cooled down by surrounding it with a Dewar flask filled with liquid air and the gas evolved during the first ten minutes was collected in it. T_1 was then sealed at the constriction. Alpert valve V_2 was then closed with a torque wrench and the stopcock S_1 was slowly opened. The gas passing through trap T_2 was purified from hydrogen fluoride (HF), which condensed at dry-ice-acetone temperature, and was collected in trap T_3 at liquid air temperature in a solid form. When enough BF_3 was collected in T_3, stopcock S_1 was closed and V_2 was opened. The system was pumped down to less than 10^{-5} mm Hg, V_2 was closed, and the liquid air surrounding T_3 was removed to evaporate the collected solid BF_3. When the BF_3 pressure, as indicated by manometer M, acquired a predetermined value, V_1 was closed. The remaining gas in the system was removed by opening stopcock S_3 and cooling T_4 down to liquid air temperature.

The counters now filled with BF_3 were heated for two hours by an infrared lamp to accelerate the reaction of BF_3 gas with the counter walls. This gas was then removed from the counters by opening V_1 and stopcock S_3 and collecting it in trap T_4. The

system was once again pumped down to less than 10^{-5} mm Hg. This procedure of filling, removing, and pumping was repeated three times before the final filling of the counters, after which the valve V_1 was closed and the counters were wrapped by wet asbestos sheets and sealed at the constrictions.

The procedure adopted for filling the counters using the modified vacuum system shown in Fig. 9 was as follows.

1. The counters were evacuated and outgassed as before and the system was checked for leaks.

2. The compound was heated to 100° C and the pumping was continued until the pressure was down to less than 10^{-5} mm Hg.

3. Alpert valve V_1 was closed and the compound was heated to between 180° and 200° C. The gas evolved during the first ten minutes was condensed in trap T_1 and T_1 was sealed at the constriction.

4. Dewar flasks containing solid CO_2 - acetone mixture and liquid air were placed around T_2 and T_3, respectively.

5. Alpert valve V_2 and stopcock S_1 were closed and V_1 was opened. The BF_3 evolved was collected in trap T_3.

6. When the desired amount of gas was collected, V_1 was closed and the system was opened to the pumps by opening stopcock S_1.

7. The system was pumped down until the pressure became less than 10^{-5} mm Hg. S_1 was closed and the counters were opened to the system by opening the valve V_2. The liquid air flask surrounding trap T_3 was slowly removed and the pressure of

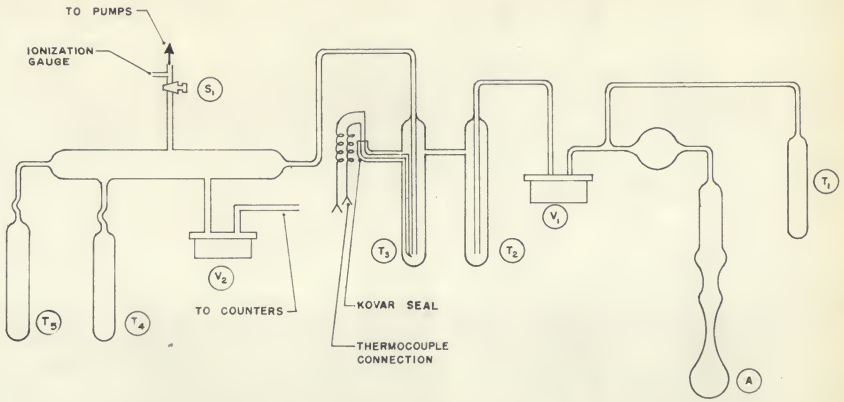

Fig. 9. Schematic diagram of modified filling system. A, 50-ml flask; T_1, T_2, T_3, T_4, and T_5, traps. S_1, glass stopcock; V_1, V_2, Alpert valves.

the gas evolved was checked on manometer M.

8. V_2 was closed and the counters were heated by infrared lamp for two hours. The gas in the system was collected in trap T_4 which was then sealed at the constriction.

9. This procedure of filling, soaking, and pumping out the BF_3 gas was repeated once more, before sealing the counters at the constriction. Every time the system was pumped down before filling, the temperature of the solid BF_3 was checked with the Cu-Constantan thermocouple located in T_3. The temperature was usually irregular for a period of time and then became constant. This could be attributed to the condensable impurities being pumped out. The filling process was never started until this constant temperature was acquired. The temperature of the evolved gas, after removal of the liquid air flask, was also checked to test the purity of the gas. Figures 10 and 11 show the variance of temperature (T) with time (t) at two different pressures. Data used in plotting the above curves are listed in Table 2.

COUNTER INSTRUMENTATION

A block diagram indicating the instrumentation generally required for the boron trifluoride proportional counter is shown in Fig. 12.

As the tube is normally located at a distance from the instrumentation, coaxial cable must be employed to transmit the pulses from the tube to the amplifier. For lengths of cable less

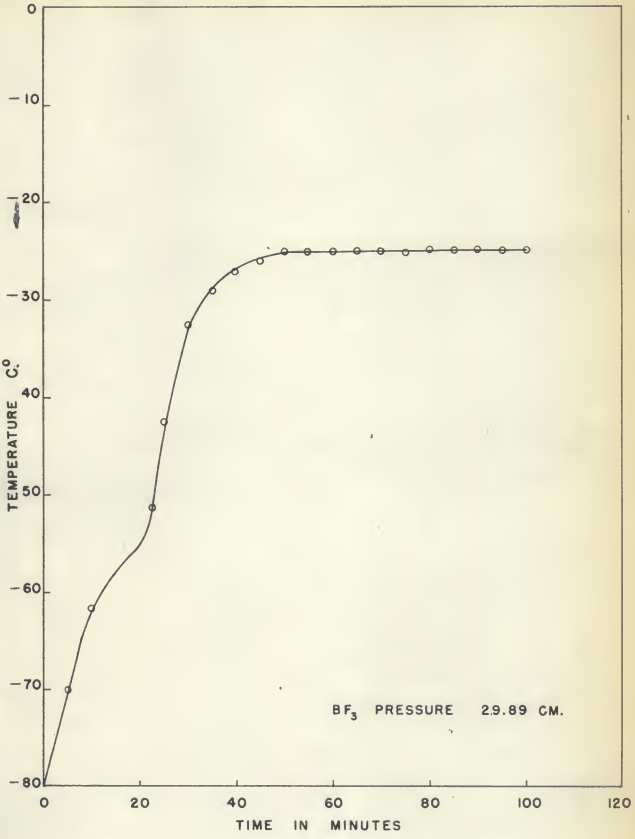

Fig. 10. Variation of BF_3 temperature with time.

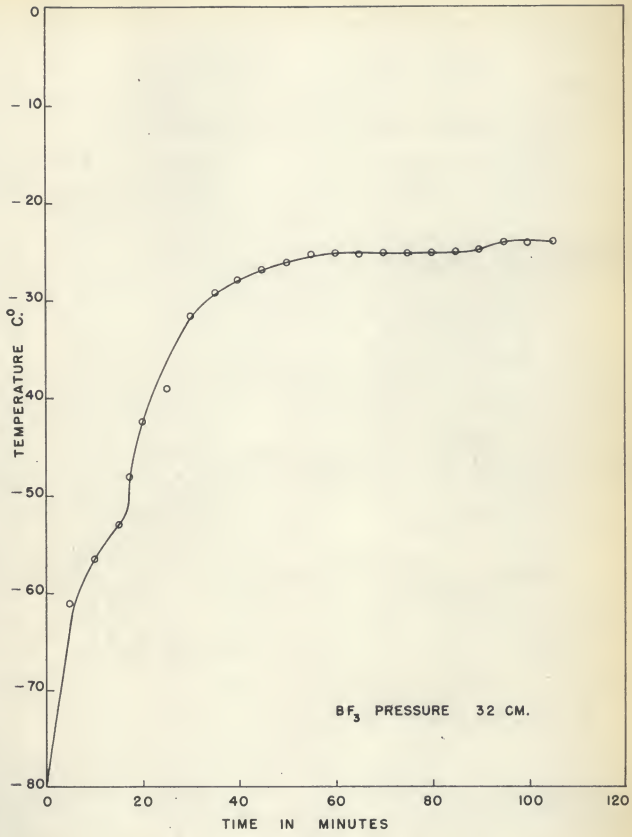

Fig. 11. Variation of BF_3 temperature with time.

Table 2. Variation of BF_3 gas temperature with time.

BF_3 pressure = 12.6 inches Hg		BF_3 pressure = 11.79 inches Hg	
t minutes	T° C	t minutes	T° C
0	-78.4	0	-78.3
5	-70.0	10	-61.0
10	-61.4	15	-50.5
15	-55.0	20	-48.0
20	-42.3	25	-42.5
25	-32.6	30	-39.0
30	-29.0	35	-31.5
35	-27.0	40	-29.3
40	-26.0	45	-28.0
45	-25.4	50	-27.5
50	-25.2	55	-26.2
55	-25.1	60	-25.2
60	-25.2	65	-25.2
65	-25.2	70	-25.2
70	-25.2	75	-25.2
75	-25.2	80	-25.2
83	-25.2	85	-25.2
85	-25.2	90	-25.2
87	-25.2	95	-25.2
		100	-24.2
		105	-24.1

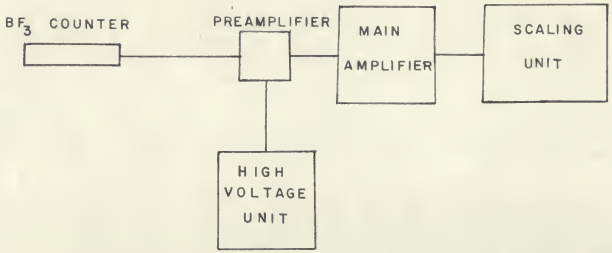

Fig. 12. BF_3 counter instrumentation.

than 25 feet, cable effects may be neglected. However, the cable capacity undesirably influences the pulse formation and transmission. For this reason, the preamplifier is located physically close to the BF_3 counter. Besides its amplification effects, the preamplifier serves the purpose of impedance transformation; that is, to transform the voltage which is developed across the small capacity at the input of the preamplifier into an approximately equal voltage across the high capacity of the output cable. The preamplifier used in this work consisted of a 404A tube which was d-c coupled to a 417-A output cathode follower. Capacity feedback could be provided to the input from either the full output or one-third or one-tenth of the output. This gave the preamplifier gain a setting of 1, 3, or 10. Since most of the time a long cable was used, the gain was maintained at 3. The entire preamplifier assembly was contained in the Detectolab Model DA 8 linear amplifier. The output of the preamplifier was coupled into the differentiating network of the main amplifier. The differentiating network of the amplifier determines the low-frequency cut-off and the clipping time of the amplifier, while the integration network determines the upper frequency cut-off of the amplifier and affects the rise and delay times of the pulses.

The resolving time of the proportional counter, which is the minimum time that can elapse between the start of two pulses if they are to be counted as two pulses, is determined by the rise of the pulses. The resolving time of the system, that is, the counter, amplifier, and scaling unit, is the result of the

composite characteristics of all the elements in it (19).

High voltage was fed directly to the preamplifier from the high-voltage power supply Model DVI, B. J. Electronics, N. E. Dept. No. 262. The preamplifier furnished the signal to the multiconductor preamplifier cable.

The gain of the linear amplifier, Model DA8, B. J. Electronics, N. E. Dept. No. 376, consisted of a coarse attenuator with six steps, each increasing the gain by a factor of 2, while the fine attenuator had a continuous control and covered a factor of one. In order to calibrate this gain dial, a known input signal was introduced from the Radiation Instruments Company pulse generator, Model 1401, N. E. Dept. No. 1046. The output pulses at each setting of the gain dial were measured on the screen of an oscilloscope, Type Tex. 545. The gain, $\frac{E_{out}}{E_{in}}$, was calculated at each setting of the gain dial and the values obtained were plotted against their corresponding dial setting in Fig. 13.

COUNTER CHARACTERISTICS

Proportional Counter Action

Theory. Consider an electron which has been formed at a certain point within the volume of the central wire by an initial ionizing event. This electron will drift towards the central wire under the influence of the field due to the applied voltage. As the electron drifts in, it will make collisions with the atoms and molecules of the gas with which the counter is filled. If

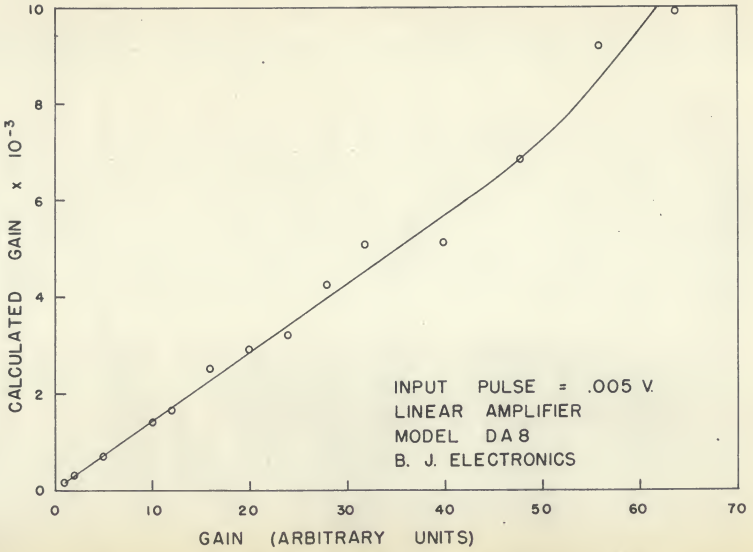

Fig. 13. Calibration of the gain dial setting on the DA8 B.J. Electronics linear amplifier, N. E. Dept. No. 376.

the counter has cylindrical geometry, the field varies inversely as the first power of the radius (19),

$$E = V_o/r \log(r_2/r_1) \qquad (7)$$

where E is the electric field strength, V_o is the applied voltage, r_1 and r_2 are the radii of the wire and cathode, respectively. From equation (7) it can be seen that the field increases towards the central wire, therefore the electron will acquire more energy per unit path near the central wire. Thus when the electron gains enough energy in one mean free path between collisions to produce ionization, the next time it hits an atom it will ionize the atom. It is thus the beginning of the process of cumulative ionization, which is the basis of the counter action. If this collision resulting in ionization takes place at some distance from the central wire, the initial electron plus the new electron will start on their next free path towards the central wire. Since the field increases nearer the wire, any electron which has acquired enough energy to produce ionization by collision at one point will acquire enough energy to ionize in subsequent mean free paths.

For a cylindrical proportional counter with two concentric electrodes, the size of the pulse V in volts appearing on the central wire system is given by (20)

$$V = A\ ne/C \qquad (8)$$

where A is the gas multiplication and n is the number of electrons in the initial ionizing event. If V is expressed in volts, then e is the charge on the electron in microcoulombs and C is the distributive capacity of the central wire system in microfarads. The gas multiplication A is defined as the number of

additional electrons produced by each initial electron and by its progeny as it travels from the place where it is originally formed to the central wire. Thus A is a measure of the size of the "avalanche" which each initial electron starts, and the avalanches are assumed to be independent of each other.

As the voltage V_o, equation (7), across the counter is slowly raised, a value is obtained at which the multiplication starts. The lowest voltage at which this occurs is the threshold voltage for a proportional counter. The physical significance of this voltage lies in the fact that it is the minimum voltage at which an electron traveling towards the central wire acquires enough energy to ionize in its last free path before it reaches the wire. If r_o is defined as the radius at which the avalanche starts, r_o will be equal to r, at the threshold voltage. However, r_o in the region of proportional counting never becomes much greater than r_1 (see discussion in Appendix), and therefore assumes an approximately linear dependence on the potential. The radius r_o, at which the avalanche starts when the voltage applied is V_o, is therefore related to the threshold voltage V_p, as follows (20):

$$r_o = r_1 V_o/V_p \qquad (9)$$

Thus r_o is defined in terms of the directly measurable voltages and wire radius.

The multiplication factor A, as defined in equation (8), is determined by the number of ionizing collisions which the electron makes as it travels to the wire. Rose and Korff (20) give the following general expression for the gas multiplication A at

an applied voltage V_o,

$$A = \exp 2 \left(a N_m C r_1 \phi(0) V_o\right)^{\frac{1}{2}} \left[(V_o/V_p)^{\frac{1}{2}} - 1\right] \quad (10)$$

where $\phi(0)$, the number of slowest electrons, is to be equal to unity (see discussion in Appendix), N_m is the number of gas molecules per unit volume, C the capacity per unit length of the counter, r_1 the wire radius, V_p the threshold voltage, and "a" is the rate of change of the ionization cross section for energies just above the ionization potential. Equation (10) can be written as

$$A = \exp k V_o^{\frac{1}{2}} \left[(V_o/V_p)^{\frac{1}{2}} - 1\right] \quad (11)$$

where $k = 2\left(a N_m C r_1 \phi(0)\right)^{\frac{1}{2}}$. This is an adequate form for calculation of the theoretical values of gas multiplication.

Experimental Values of Gas Multiplication. The experimental values of multiplication for counter (B), Fig. 4, were determined using the circuit shown in Fig. 14.

The procedure for measuring the gas multiplication was as follows:

1. The linear amplifier, Model DA 8, B. J. Electronics, N. E. Dept. No. 376, gain was reduced to a minimum and the high voltage increased until pulses appeared on the oscilloscope screen.

2. The pulse height-selector setting dial was increased slowly until no pulses were visible on the oscilloscope screen. The PHS reading together with the corresponding high voltage and the linear amplifier gain were noted.

3. Voltage was reduced in steps of 50 volts, gain was adjusted if necessary, and at each voltage setting, step 2 was

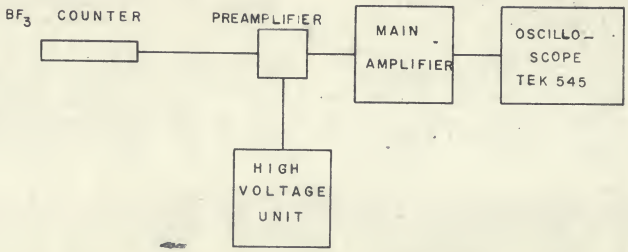

Fig. 14. Block diagram of the equipment needed for measuring gas multiplication.

repeated.

4. The maximum pulse height corresponding to an arbitrarily selected point in the plateau region of the counter was noted.

5. The PHS readings obtained at the different voltage settings were renormalized to the same gain. The data so obtained was renormalized to a multiple of the pulse height obtained in step 4. Values of the pulse sizes thus obtained are included in Table 3 and plotted against the corresponding voltages in Fig. 15.

From Fig. 15 it is seen that the pulse size is approximately constant between 550 and 750 volts. Considering that the counter was acting as an ionization chamber in this region, that is, the multiplication in this region was unity, the absolute multiplication values were obtained by normalizing the arbitrary pulse sizes obtained at different voltages by the constant pulse size obtained in this region. Multiplication values thus obtained are listed in Table 4 and plotted versus voltage in Fig. 16.

The threshold voltage V_p is the voltage corresponding to the point where the straight-line portion of the curve, Fig. 16, if extrapolated downwards, would intersect the abscissa. The observed value for V_p is 855 volts. The theoretical value of V_p was calculated from equation (11) by considering the first two points lying on the straight-line portion of the curve, Fig. 16, as follows.

If A_1 and A_2 are the multiplication factors at these two

Table 3. Pulse height and gas multiplication data.

High voltage	PHS readings (arbitrary units)	Gain	Normalized PHS readings to gain one	Renormalized to multiple of the PHS reading on counter plateau	Pulse size (arbitrary units)
1750	1.910	1	1.910	0.3410	341.00
1700	1.495	1	1.495	0.2670	267.00
1650	2.420	2	1.210	0.2160	216.00
1600	2.130	2	1.065	0.1902	190.00
1550	1.665	2	0.833	0.1487	148.70
1500	1.515	2	0.757	0.1351	135.10
1450	1.280	2	0.640	0.1142	114.20
1400	1.860	4	0.465	0.0830	83.00
1350	1.450	4	0.362	0.0646	64.60
1300	2.040	8	0.255	0.0455	45.50
1250	1.400	8	0.176	0.0312	31.20
1200	0.900	8	0.112	0.0200	20.00
1150	1.170	16	0.070	0.0125	12.50
1100	0.845	16	0.052	0.0093	9.30
1050	0.725	16	0.045	0.0081	8.10
1000	0.965	32	0.031	0.0055	5.50
950	0.930	32	0.028	0.0050	5.00
900	0.840	32	0.026	0.0046	4.60
850	0.775	32	0.022	0.0039	3.90
800	0.700	32	0.021	0.0037	3.70
750	0.650	32	0.019	0.0035	3.50
700	0.600	32	0.015	0.0035	2.30
650	1.600	64	0.012	0.0023	2.10
600	1.150	64	0.010	0.0021	2.10
550	1.100	64	0.009	0.0017	1.78

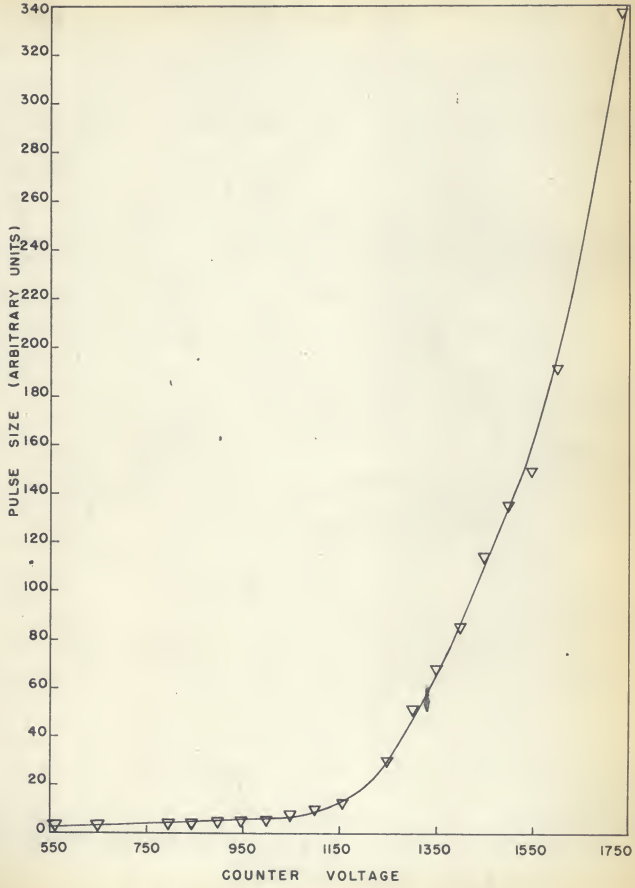

Fig. 15. Relative pulse size versus corresponding voltage.

Table 4. BF_3 gas multiplication data.

High voltage	Normalized PHS readings	Multiplication
1750	0.341	191.001
1700	0.267	149.520
1650	0.216	120.960
1600	0.190	106.512
1550	0.148	83.272
1500	0.135	76.600
1450	0.114	63.952
1400	0.083	46.480
1350	0.064	36.176
1300	0.045	25.480
1250	0.031	17.472
1200	0.020	11.200
1150	0.012	7.000
1100	0.009	5.408
1050	0.008	4.536
1000	0.005	3.096
950	0.005	2.800
900	0.004	2.598
850	0.003	2.200
800	0.003	2.100
750	0.003	1.971
700	0.003	1.843
650	0.002	1.277
600	0.002	1.199
550	0.001	1.000

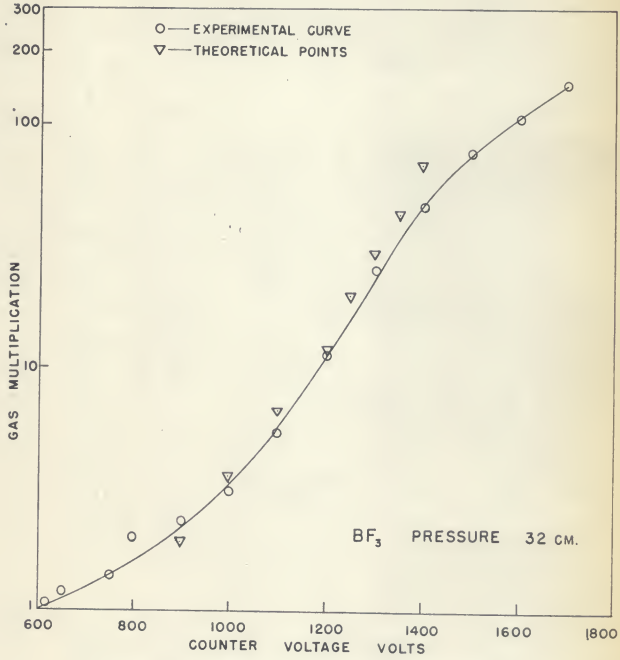

Fig. 16. Effect of counter voltage on gas multiplication.

points, V_1 and V_2 are the corresponding voltage values,

$$A_1 = \exp k\, V_1^{\frac{1}{2}} \left[(V_1/V_p)^{\frac{1}{2}} - 1\right]$$

$$A_2 = \exp k\, V_2^{\frac{1}{2}} \left[(V_2/V_p)^{\frac{1}{2}} - 1\right]$$

Therefore $$\frac{\ln A_1}{V_1^{\frac{1}{2}}\left[(V_1/V_p)^{\frac{1}{2}} - 1\right]} = \frac{\ln A_2}{V_2^{\frac{1}{2}}\left[(V_2/V_p)^{\frac{1}{2}} - 1\right]}$$

Using this equation, the calculated value of V_p was 795.5 volts. From equation (11) it can be seen that k is a constant depending on the nature and pressure of the gas and on the wire and cylinder radii. k also depends on the energy distribution of the secondary electrons arising in the avalanche process. In the approximation made in deriving equation (10), the relative number of slowest electrons enters and is adjusted in the parameter a. Since no information as to the availability of data on a for BF_3 was present, the value of k was calculated at one voltage V_o by using the theoretical V_p value and known multiplication factor A. Using this method, the value of k, calculated to be 0.034089, was used to calculate the theoretical values of multiplication at different voltages. Theoretical values of multiplication obtained as such are listed in Table 5 and plotted in Fig. 16.

It is to be noted that equation (11) predicts that values of log A corresponding to different V_o values, contrary to Fig. 16, should lie on a straight line of slope $(d \log A/dV_o)$.

This disagreement is apparent, however, only when one takes into consideration the assumption on which the derivation of equation (10) is based. The assumption of interest in the present connection involves neglecting of fluctuations in energy loss, as

Table 5. Theoretical values of multiplication for k = 0.034089 and V_p = 799.5 volts.

High voltage	$k(V_n)^{\frac{1}{2}}\left[(V_n/V_p)^{\frac{1}{2}} - 1\right]$	$\exp k(V_n)^{\frac{1}{2}}\left[(V_n/V_p)^{\frac{1}{2}} - 1\right]$	A
900	0.65839	1.9348	1.9348
1000	1.21444	3.3535	3.3535
1100	1.92455	6.8210	6.8210
1200	2.47300	11.8123	11.8123
1250	3.05520	21.2223	21.2223
1350	3.78240	43.8160	43.8160
1400	4.16880	64.7150	64.7150

it is assumed that at a given cylinder voltage there exists a point at a distance r_o from the wire axis at which the avalanches start, and that this distance is the same for all electrons initiating such avalanches. The value of r_o which was used in obtaining equation (10) was, in fact, the average starting point for sustained ionization. While this assumption would be expected to be valid for large voltages, for which the mean r_o is considerably greater than the wire radius r_1, it should also be expected that it will break down at low voltages. This is immediately evident when one considers the effect of a distribution in starting points r_o which would naturally enter as an essential component of the avalanche model when fluctuations are taken into account.

At low voltages the gas multiplication is, at first, caused by these few electrons which have large r_o. As the voltage is increased, the r_o distribution function shifts outward from the wire until it is virtually outside the point r_1 so that practically all the electrons contribute to the multiplication. Therefore the amount of charge collected when gas multiplication sets in, and hence the multiplication itself, would increase more slowly than if all avalanches started at the same point and a curve of the sort obtained (d log A/dV or dA/dV = 0 for A = 1) would be expected.

Hence it can be stated that the form of the multiplication curve near the threshold is to a certain extent a picture of the r_o distribution function for r_o larger than the average value. Therefore at higher voltages when all but a small portion of r_o

distribution function lies outside r_1, almost all the primary electrons are effective in initiating avalanches. Thus the assumption of a fixed r_o, while not rigorously fulfilled, gives an asymptotic value of A in equation (11) for very large voltages.

Sensitivity of Boron Trifluoride Counters

Theory. The B^{10} (n, α) reaction has been studied quite extensively by Brower, Bretscher, and Yilhent (8). The reaction is exothermic, with an energy release of 2.78 mev. The ground state of the Li^7 product nucleus may be formed directly, with the entire energy being shared by the Li^7 and the alpha particle. Alternatively, an intermediate excited state of Li^7 may be formed, followed by the emission of a 0.48 mev gamma. The probability of reaching the ground state directly is only 0.07 for reactions induced by thermal neutrons. It rises to a maximum of about 0.7 for 1.8 mev neutrons, followed by a drop to less than 0.5 for 2.5 mev neutrons (18).

For the capture of a neutron of energy E, the kinetic energy, E_{ke}, of either E + 2.30 mev or E + 2.78 mev will be shared by the alpha particle and the lithium recoil nucleus. If the captured neutron is thermalized, E is approximately zero, and the energies of the lithium nucleus and the alpha particle in this case are (19):

$$E_{Li} = \frac{E_{ke}\, M_{\alpha}}{M_{\alpha} + M_{Li}} = \frac{(2.30)(4.00)}{4.00 + 7.02} = 0.88 \text{ mev}$$

and

$$E_{\alpha} = \frac{E_{ke}\, M_{Li}}{M_{\alpha} + M_{Li}} = 1.47 \text{ mev}$$

where M_{α} and M_{Li} are the mass of α-particle and Li-nucleus, respectively.

The energy dependence of the cross section σ for the B^{10} (n, α) reaction was found to vary inversely with the velocity to about 100 ev, and therefore can be represented mathematically as

$$\sigma = \frac{\sigma_o\, v_o}{v} \qquad (12)$$

where σ_o is the cross section of the reaction of B^{10} atoms with the thermal neutrons at room temperature, having a value of 4,010 barns, and v_o is the velocity of thermal neutrons at 293° K with a value of 2.2×10^5 cm per second.

The reaction rate in such a detector can be obtained by (19):

$$R = \frac{n\, v}{\lambda} = n\, v \Sigma = \phi \Sigma$$

where n is the number of neutrons per cubic centimeter, R is the reaction rate per cubic centimeter, ϕ and Σ are the neutron flux and the total cross section of B^{10} (n, α) reaction. The contribution dR to the reaction rate by neutrons between E and E + dE in the volume dV is

$$dR = N(X, Y, Z)\, \phi(E, X, Y, Z)\, \sigma(E)\, dE dV$$

where N(X, Y, Z) is the number of B^{10} atoms per unit volume at point X, Y, Z, $\sigma(E)$ is the cross section at energy E, and $\phi(E, X, Y, Z)$ is the neutron flux per unit energy interval at the point X, Y, Z.

The total reaction rate throughout the entire detector could be represented by the integral over the detector volume and the complete neutron-energy spectrum, and can be written as

$$\text{Reactions per second} = \int_{\text{vol}} \int_{0}^{\infty} N(X, Y, Z)\, \sigma(E)\, \phi(E, X, Y, Z)\, dV dE \qquad (13)$$

If the flux can be considered independent of the position in the detector, and if the total number of B^{10} nuclei can be represented by N_T, equation (13) becomes

$$\text{Reactions per second} = N_T \int_{0}^{\infty} \sigma(E)\, \phi(E)\, dE \qquad (14)$$

For a neutron spectrum between 0 and 100 ev, equation (12) can be applied and equation (14) becomes (19)

$$\text{Reactions per second} = N_T\, \sigma_o\, v_o \int_{0}^{100\ \text{ev}} n(E)\, dE$$

$$= N_T\, \sigma_o\, v_o\, n \qquad (15)$$

where n is the number of neutrons per unit-volume, irrespective of energy up to 100 ev. If P(E) represents the probability that a B^{10} (n, α) reaction caused by a neutron of energy E will register a count, then from equation (15) the expression for the counting rate is

$$\text{Counts/sec} = NV\, \sigma_o\, v_o \int_{0}^{\infty} P(E)\, n(E) dE \qquad (16)$$

where $N_T = NV$, that is, the product of the density of $B^{10}F_3$ atoms and the volume of the detector.

In most cases, the counter is used with a counting system that requires a certain minimum pulse size for it to be triggered.

This means that the total energy of the alpha particle and the lithium nucleus dissipated in the chamber should exceed a certain threshold value E_t. Since in practice the chamber dimensions are usually larger than the particle ranges and the threshold energy E_t is much less than the total energy available, the probability function P(E) can be taken as 1 to a good approximation.

If the sensitivity of a counter is defined as the counts per second per unit neutron flux, the expression for sensitivity as given by equation (16) is

$$\text{Sensitivity} = NV\ \sigma_o\ (v_o/\bar{v}) \qquad (17)$$

For Maxwell-Boltzman distribution, this becomes

$$\text{Sensitivity} = \frac{4{,}010 \times 10^{-24}\ NV}{1.128}$$

where $\bar{v} = 1.128\ v_o$, N is the total number of B^{10} atoms per cubic centimeter, and V is the sensitive volume of the counter. Equation (17) is valid only if the flux is constant throughout the counter volume.

Experimental Determination of Sensitivity. The experimental value of the sensitivity was determined by placing the counter at different positions in the Kansas State University graphite subcritical assembly. Positions of the slots and source are shown in Fig. 17. This pile consists of a rectangular parallelepiped 68 inches square and 100 inches high, which rests on a concrete foundation. Machined reactor grade graphite blocks, about four inches in cross section and of various lengths, were used to construct the column. Some of the graphite blocks, as shown in Fig. 17, were drilled to a diameter of 1.75 inches along the

Fig. 17. Kansas State University subcritical assembly.

length of the block to accommodate fuel slots. Each of these fuel slots contained graphite cylinders measuring 1.625 inches in diameter and 22.68 inches in length. These cylinders, called plugs, are made of the same material as the graphite blocks.

For the standardization of counter (B), Pu-Be neutron source #3761, containing about 16 gms of Pu and emitting approximately 1.71×10^6 neutrons per second, was placed in the center of fuel port 1, Fig. 17. Accurate determination of the flux distribution in the graphite pile using indium foils and small commercial BF_3 counters was carried out by Foulke (12), using a Pu-Be source emitting 1.58×10^6 neutrons per second. A conversion factor of 1.0823 was therefore used to correct for the difference in the source strengths.

The counter was connected directly to a Nuclear Chicago preamplifier, Model 1062, N. E. Dept. No. 96, output of which was fed to a Baird atomic scaling unit, Model 132, N. E. Dept. No. 145. A regulated high-voltage supply, John Fluke Model 400BDA, N. E. Dept. No. 179, was used as the high-voltage source for the counter.

The measurements were run so as to give 10,000 counts in each position. The count rates were corrected for background and listed in column 4 of Table 6. The experimental values of sensitivity at each position of the pile were independently calculated. Values obtained are given in column 5 of Table 6, and plotted against distance from source in Fig. 18. From this figure it can be seen that the sensitivity increases with the increase in distance up to about 1.5 diffusion lengths and then remains

Table 6. Variation of sensitivity of counter (B) with change in distance between counter and source.

Distance from source, cm	Flux*, neutrons per cm^2 per sec	Flux** neutrons per cm^2 per sec	Counts per second	Sensitivity, counts per sec per unit flux
20.32	1910	2067	175.586	0.084947
40.64	1290	1397	123.783	0.088606
60.96	720	770	73.206	0.095073
81.28	379	410	39.696	0.096818
101.60	189	214	20.633	0.096417
121.92	102	110	10.613	0.096484

*These data were determined by L. Foulke (12) using indium foil technique.

**Corrected for the difference in source strength.

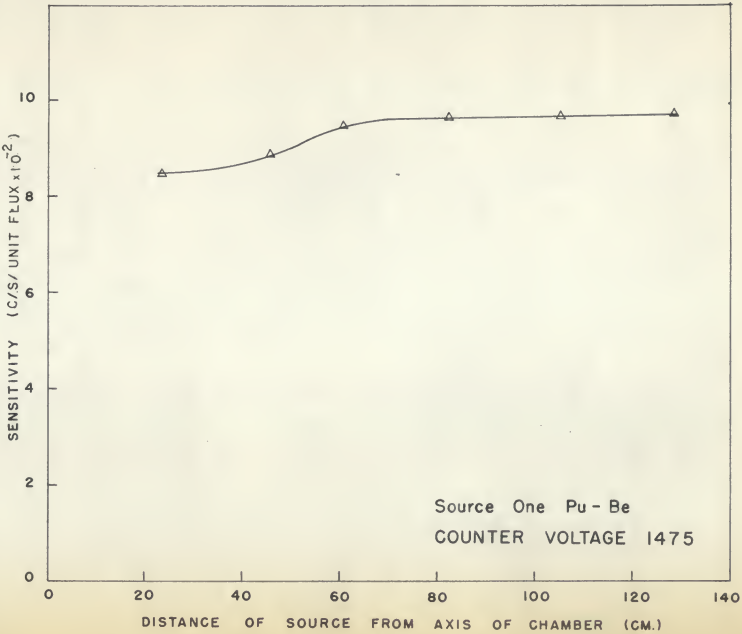

Fig. 18. Counter sensitivities measured at different distances from the source.

constant. Experiments done in this department on the graphite assembly show that the Cadmium Ratio, defined as the ratio of total flux to epicadmium flux, rises sharply at approximately 1.5 diffusion lengths from the source which, for graphite, corresponds to about 75 cm. Thus the increase of sensitivity with the increase in distance can be attributed to the fact that at smaller distances neutrons are not thermalized enough and that the cross section of B^{10} (n, α) reaction is correspondingly lower.

Equation (17) was used to calculate the sensitivity of the counter as such:

Pressure of BF_3 gas inside the counter = 29.9 cm Hg

Sensitive length = 5 inches

Diameter of the cylinder = 0.94 inch

Sensitive volume = $\pi R^2 h$ = 56.8079 cm^3

The sensitive volume has been calculated here on the assumption that it is a rectangular cylinder. Since the central wire was supported at one end by a thicker metal rod, the field strength at the surface of the wire is weaker near this end and reaches its normal value only at some distance from this end (19). The field near the end is therefore different from the field near the center and the lines of forces are not radial so that the sensitive volume is not a rectangular cylinder but has a conical shape near this end. Since the boron trifluoride gas was 96 per cent enriched in B^{10} component, the density N of the B^{10} atoms in the counter was:

$$N = \frac{(6.02 \times 10^{23})(\text{atoms/gm atom})(29.96)(\text{pressure, cm Hg})(0.96)\,(\text{atoms } B^{10}/\text{total atoms})}{(76)(\text{atmospheric pressure, cm Hg})(22.4 \times 10^{3})(\text{cm}^3/\text{gm mole})}$$

$$= 9.8954 \times 10^{18} \text{ atoms per cm}^3$$

Substituting the value of V and N in equation (17),

$$\text{Sensitivity} = \frac{(4010 \times 10^{-24}\, NV)}{1.128}$$

$$= \frac{4010 \times 10^{-24}(0.9895 \times 10^{19})(56.8079)}{1.128}$$

$$= 1.998 \text{ counts per unit neutron flux per second}$$

Comparison of this result with the experimental values in Table 6 shows that the latter are between 4 and 5 per cent of the theoretical values. This discrepancy can be attributed to several factors, among which are the inaccuracy in determining the sensitive volume (19), the thickness of the anode wire (19), the gas impurities (4), and the electronic circuitry.

Plateau and Integral Bias Curves

Some typical curves of counting rate versus voltage applied to the counter are shown in Figs. 19 and 20. The neutron source used to obtain these data were a Pu-Be source moderated in paraffin. A linear amplifier, type DA8, B. J. Electronics, N. E. Dept. No. 364, in conjunction with a scaler DS9, B. J. Electronics, N. E. Dept. No. 144, formed the electronic circuit. The counter was connected to the preamplifier through a coaxial cable type RG11-U. Figures 19 and 20 show the effect of amplifier gain

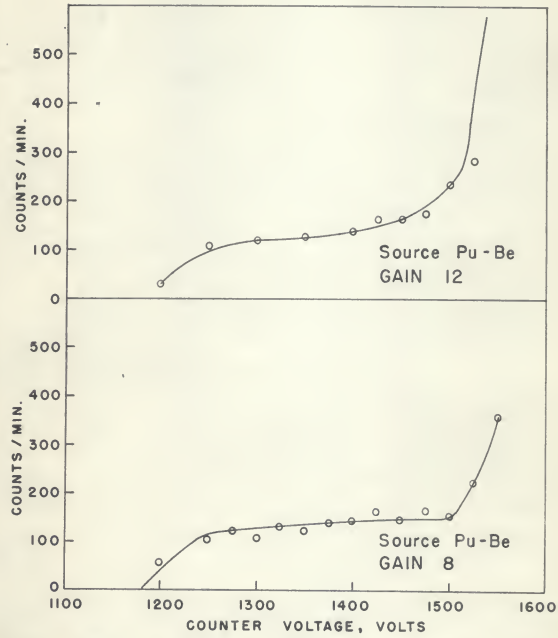

Fig. 19. Effect of gain on the plateau of the BF_3 counter.

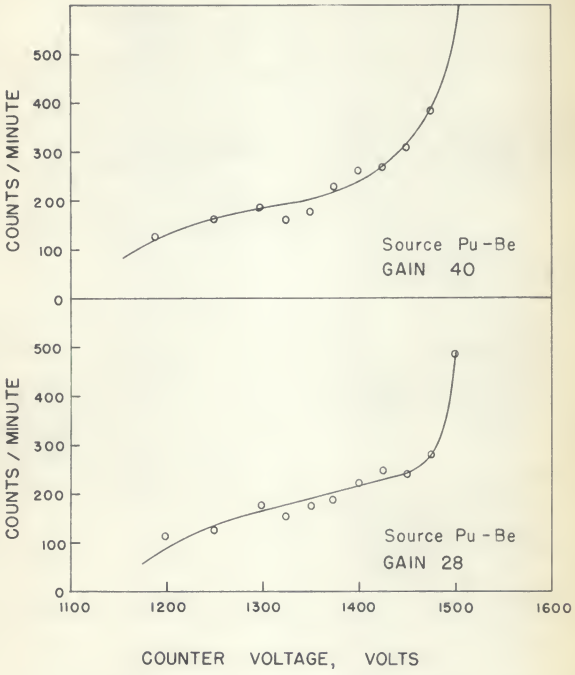

Fig. 20. Effect of gain on the plateau of the BF_3 counter.

on the plateau characteristics. As shown in Fig. 19, the plateau is about 250 volts at a gain of 8; however, it becomes shorter and steeper with higher gain.

An integral bias curve with 1475 volts applied to the counter is shown in Fig. 21. The relatively broad distribution in the count rate is attributed to the partial ionization loss by the disintegration products which strike the wall of the counter. The geometry is favorable for the production of these small pulses since the range of the disintegration product is of the order of half the counter radius. If the ratio of range to the counter radius were decreased by using a larger diameter or higher filling, the effect would be considerably reduced. However, at the same time the sensitivity to the gamma radiation would be increased, an important consideration for reactor application.

Effect of Gamma Rays on the Counter Performance

In order to determine the relative efficiency of the counter for gamma rays as compared to its efficiency for neutrons, and, further, to determine the effect of the amplifier gain on this relative efficiency, the following experiment was performed.

1. The counter was placed at a fixed distance from Nuclear Chicago moisture gauge, Model P-21, N. E. Dept. No. 136, containing five-millicurie Ra-Be source surrounded by paraffin to provide a beam of thermal neutrons. Counts were taken at several 5-minute intervals at a certain setting on the amplifier. The average count rate corresponding to that particular gain

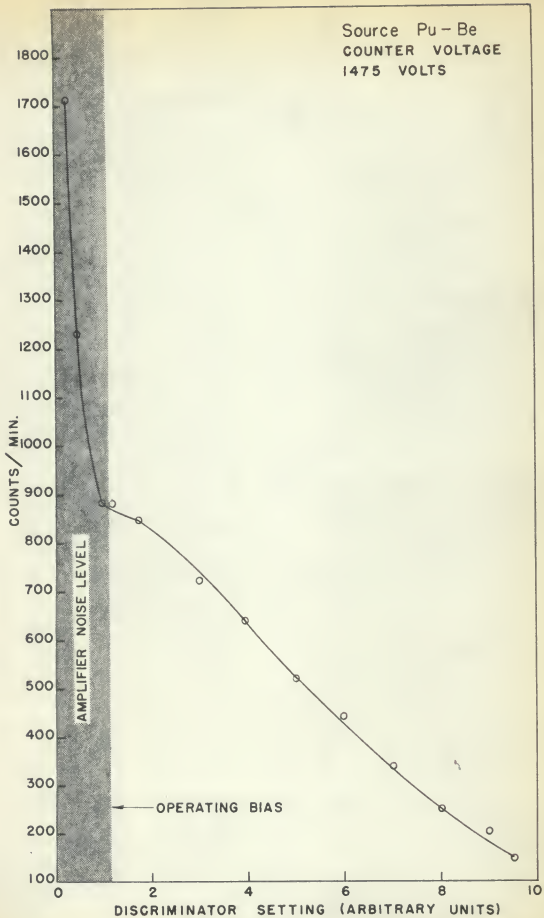

Fig. 21. Integral bias curve for BF_3 counter.

setting was determined, corrected for background, and recorded in column 3 of Table 7. Background and background plus neutron count rates are plotted versus gain dial setting in Fig. 22.

2. The dose rate received by the counter from the source was determined by placing a slow-fast survey meter, Model RCL 20806, N. E. Dept. No. 10178, at the same distance from the source. The dose rate obtained in this case was 0.0046 mr per hour.

3. Procedure adopted in step 1 was repeated for gamma rays. Source used in this experiment was a Cs-137 one, and placed at four inches from the counter. The average count rate versus gain dial setting on the amplifier is plotted in Fig. 22, and the values corrected for background are listed in column 2 of Table 7.

4. The dose rate received by the counter from the gamma ray source was determined by a GM survey meter, SM-136, serial 1408, N. E. Dept. No. 10156. The value obtained was 6.5307 mr per hour, at four inches from the source.

5. Count rate values for neutrons and gamma rays were normalized to the same source strength and listed in columns 5 and 4 of Table 7.

6. The normalized gamma counts were divided by the corresponding normalized neutron readings to determine the relative counter efficiencies. Results are listed in column 6 of Table 7 and plotted in Fig. 23 against the corresponding gain settings in column 1. Figure 23 shows that the relative counter efficiency for gamma rays increases with the increase in gain. This can be

Table 7. Relative efficiency of BF_3 counter for gamma rays.

Gain	Gamma counts per five minutes	Neutron counts per five minutes	Normalized gamma counts	Normalized neutron counts	Relative gamma efficiency
1	17.5	107.5	2.679	23.36×10^3	1.146×10^{-4}
3	22.5	150.0	3.445	32.608×10^3	1.056×10^{-4}
4	30.5	155.0	4.593	33.695×10^3	1.363×10^{-4}
6	37.5	149.5	5.792	28.695×10^3	2.001×10^{-4}
8	70.0	155.5	10.718	33.696×10^3	3.181×10^{-4}
10	105.0	160.5	16.077	34.782×10^3	4.622×10^{-4}

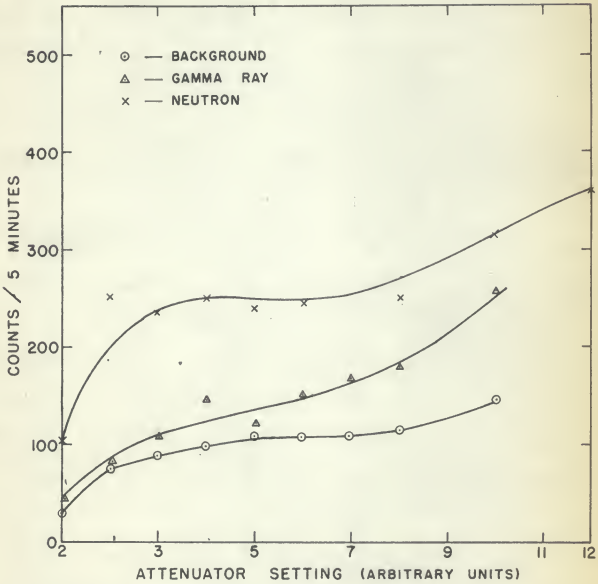

Fig. 22. Effect of amplifier gain setting on count rate of Cs-137 gammas and Ra-Be neutrons.

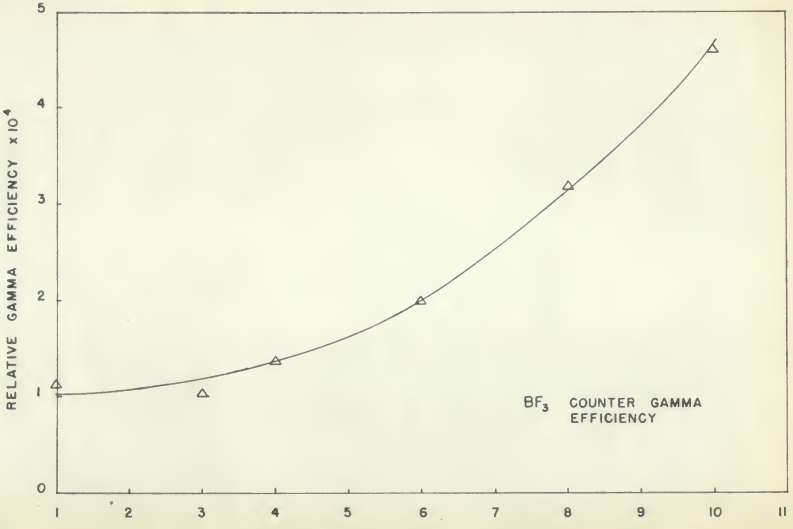

Fig. 23. Relative counter efficiencies for gammas at different gain settings.

attributed to the fact that the average pulse height produced by a gamma ray is of the order of one-hundredth of the pulse height produced by a thermal neutron. At low gains the scaler cannot see the γ pulses, but at higher gain the gamma pulses are amplified enough to trigger the scaler, and therefore a higher number of counts due to gammas is recorded.

USE OF THE COUNTER IN DETERMINING THE DIFFUSION LENGTH OF THERMAL NEUTRONS IN THE KANSAS STATE UNIVERSITY GRAPHITE MODERATED SUBCRITICAL REACTOR

Theory

The relationship between the thermal diffusion length and the thermal flux distribution in a homogeneous moderating medium according to a monoenergetic model is given by (11),

$$\nabla^2 \phi - \frac{\phi}{L^2} = 0 \qquad (18)$$

where ϕ is the thermal neutron flux, and L is the diffusion length. Equation (18) is valid for the thermal flux in regions far enough from the source so that there is no production of thermal neutrons, and a few mean free paths from the boundaries of the pile. The solution of equation (18) is given by (11),

$$\phi = \sum_{m=1}^{\infty} \sum_{n=1}^{\infty} A_{mn} \cos \frac{m\pi x}{a} \cos \frac{n\pi y}{b} \sinh \gamma_{mn} (c - z) \qquad (19)$$

where a and b are the effective x and y dimensions of the pile, respectively, c is the effective pile height measured from the

source plane, z is the distance from the source plane, $1/\gamma_{mn}$ is the relaxation length of thermal neutrons of the mn th harmonic in the z-direction given by,

$$\gamma_{mn}^2 = \frac{1}{L^2} + \left(\frac{m\pi}{a}\right)^2 + \left(\frac{n\pi}{b}\right)^2 \qquad (20)$$

and A_{mn} is a function of the assumed neutron source boundary condition in the pile. Considering a point thermal neutron source emitting S neutrons per second, and represented by a Dirac delta function, the center of source plane being taken as the center of the coordinate system, A_{mn}, is given by (11)

$$A_{mn} = \frac{2\,S}{abD\,\gamma_{mn}\cosh\gamma_{mn}\,c} \qquad (21)$$

where D is the diffusion coefficient of thermal neutrons in the lattice.

Combining equations (19) and (21) and rearranging terms, the solution of equation (18) can be written in the form (11),

$$\phi(x,\,y,\,z) = \frac{2\,S}{abD} \sum_{m=1,3,5,\ldots}^{\infty} \sum_{n=1,3,5,\ldots}^{\infty} \frac{1}{\gamma_{mn}} \cos\frac{m\pi x}{a} \cos\frac{n\pi y}{b} \frac{\sinh\gamma_{mn}(c-z)}{\cosh\gamma_{mn}\,c} \qquad (22)$$

By rewriting $\sinh\gamma_{mn}(c-z)$ in exponential form and rearranging terms, equation (22) can be written as (15),

$$\phi(x,\,y,\,z) = \frac{2\,S}{abD} \sum_{m=1,3,5,\ldots}^{\infty} \sum_{n=1,3,5,\ldots}^{\infty} \frac{1}{\gamma_{mn}} \cos\frac{m\pi x}{a} \cos\frac{n\pi y}{b}\, e^{-\gamma_{mn}z} \times \left[\frac{1 - e^{-2\gamma_{mn}(c-z)}}{1 + e^{-2\gamma_{mn}\,c}}\right] \qquad (23)$$

By expanding equation (23), the expression for $\phi(x,\,y,\,z)$ can be

written as,

$$\phi(x,\ y,\ z) = \frac{2\ S}{abD}\left[\left\{\frac{1}{\gamma_{11}}\cos\frac{\pi x}{a}\cos\frac{\pi y}{b}\,e^{-\gamma_{11}z}\ (\text{FMECF})\right\}\right.$$
$$+\sum_{m=1}^{7}\sum_{n=1}^{7}\ \frac{1}{\gamma_{mn}}\cos\frac{m\pi x}{a}\cos\frac{n\pi y}{b}\,e^{-\gamma_{mn}z}$$
$$(\text{except } 1,1)$$
$$\left.\left(\frac{1 - e^{-2\gamma_{mn}(c-z)}}{1 + e^{-2\gamma_{mn}\,c}}\right)\right] \qquad (24)$$

where FMECF is the Fundamental Mode End Correction Factor and is written in the form (15),

$$\text{FMECF} = \left(\frac{1 - e^{-2\gamma_{11}(c-z)}}{1 + e^{-2\gamma_{11}\,c}}\right) \qquad (25)$$

Equation (24) can be rearranged as follows:

$$\phi(x,\ y,\ z) = \frac{2\ S}{abD}\left[\left\{\frac{1}{\gamma_{11}}\cos\frac{\pi x}{a}\cos\frac{\pi y}{b}\,e^{-\gamma_{11}z}\ (\text{FMECF})\right\}\right.$$
$$x\left\{1 + \frac{\gamma_{11}\,e^{\gamma_{11}z}\,(1 + e^{-2\gamma_{11}\,c})}{\cos\frac{\pi x}{a}\cos\frac{\pi y}{b}\left(1 - e^{-2\gamma_{11}(c-z)}\right)}\right.$$
$$\sum_{m=1}^{7}\sum_{n=1}^{7}\ \cos\frac{m\pi x}{a}\cos\frac{m\pi y}{b}$$
$$(\text{except } 1,1)$$
$$\left.\left.\frac{e^{-\gamma_{mn}z}}{\gamma_{mn}}\left(\frac{1 - e^{-2\gamma_{mn}(c-z)}}{1 + e^{-2\gamma_{mn}\,c}}\right)\right\}\right] \qquad (26)$$

The above equation can be put in the form (15),

$$\phi(x,y,z) = \frac{2\ S}{abD}\left[\left\{\frac{1}{\gamma_{11}}\cos\frac{\pi x}{a}\cos\frac{\pi y}{b}\,e^{-\gamma_{11}z}\ (\text{FMECF})(\text{CEHCF})\right\}\right] \qquad (27)$$

where CEHCF is the Composite End and Harmonic Correction Factor and is given by (15),

$$\text{CEHCF} = \left[1 + \frac{\gamma_{11}\, e^{\gamma_{11} z}}{\cos\frac{\pi x}{a}\cos\frac{\pi y}{b}\left(1 - e^{-2\gamma_{11}(c-z)}\right)} \sum_{m=1}^{7}\sum_{n=1}^{7}{}_{(\text{except } 1,1)} \frac{e^{-\gamma_{mn} z}}{mn}\left(\frac{1 - e^{-2\gamma_{mn}(c-z)}}{1 + e^{-2\gamma_{mn} c}}\right) \cos\frac{m\pi x}{a}\cos\frac{n\pi y}{b}\right] \tag{28}$$

The thermal diffusion length is related to the relaxation length by (11),

$$\frac{1}{L^2} = \gamma_{11}^2 - \pi^2\left(\frac{1}{a^2} + \frac{1}{b^2}\right) \tag{29}$$

The diffusion length L is calculated from the flux data taken along the z-axis of the pile by using equations (24) to (28). The general procedure for calculating L is as follows.

1. A provisional value of γ_{11} is obtained from the linear slope of the ln $\phi(z)$ against z curve for points not too near the neutron source or the top of the subcritical.

2. With this value of γ_{11}, the γ_{mn}, FMECF, and CEHCF are calculated, using equations (20), (25), and (28), respectively.

3. A new value of γ_{11} is then computed from a least squares fit of flux data corrected by equation (27).

4. With this new value of γ_{11}, the process is repeated until the value of γ_{11} calculated from equation (27) coincides with the value used to calculate CEHCF and FMECF.

5. The value of γ_{11} thus obtained is used to calculate

the diffusion length using equation (29).

To eliminate tedious computations, the above procedure has been programmed through the 7th harmonics for the IBM 650 digital computer by Kaiser (15). This program was used to calculate the diffusion length using data obtained by the author.

Experimental

Experimental determination of the diffusion length L was carried out as follows.

Five one-curie (Pu-Be) sources encapsulated in tantalum and stainless steel, emitting approximately 8.0 x 10^6 neutrons per second, were placed in the Kansas State University subcritical assembly.

The BF_3 counter was connected directly to a Nuclear Chicago preamplifier, Model 1062, N. E. Dept. No. 96, and was placed in the center of each fuel port, as shown in Fig. 17. Count rates C(z) at the different z positions were found by determining the counting time for 10,000 preset counts, and were recorded in column 2 of Table 8.

ln C(z) values were plotted against z in Fig. 24 and the value of γ_{11} obtained was 0.06810 cm^{-1}. This value of γ_{11} was used in the last section.

The extrapolated dimensions of the pile a and b were determined by

$$a = a_o + 2(0.71)\lambda t$$

where a_o is the actual dimension of the pile and λ_t is the

Table 8. Data for diffusion length measurement.

Distance from source, z inch	Counts per minute	CEHCF	FMECF	Corrected counts per minute
20	18976.40	...	...	...
28	11687.40	...	...	...
36	6586.40	1.086107	0.9998805	6064.9507
44	3534.40	1.046538	0.9995840	3378.6340
52	1856.40	1.025585	0.9985539	1812.7089
60	986.62	1.014250	0.9949738	977.6714
68	587.66	1.008077	0.9825354	593.3133
76	259.65	1.004756	0.9393219	275.1142
84	110.65	1.003091	0.7891815	140.1554
92	18.71	...	...	...

L = 57.322 cm $\pm$? (One set of such data only was taken.)

transport mean free path. With $a_o = b_o = 172.448$ cm and $\lambda_t = 2.46$, the extrapolated dimensions are 175.941 cm.

Corrected values of the count rate are listed in column 5 of Table 8. Values of the CEHCF and FMECH are listed in columns 3 and 4 of the same table. Count rates obtained at points very near and very far from the sources were neglected in the IBM 650 calculations. Points lying on the straight-line portion of Fig. 24 were the only ones considered. The L value obtained was 57.32 cm based on one single set of data.

Kaiser (15) reported an L value of 52.72 cm, based on a more

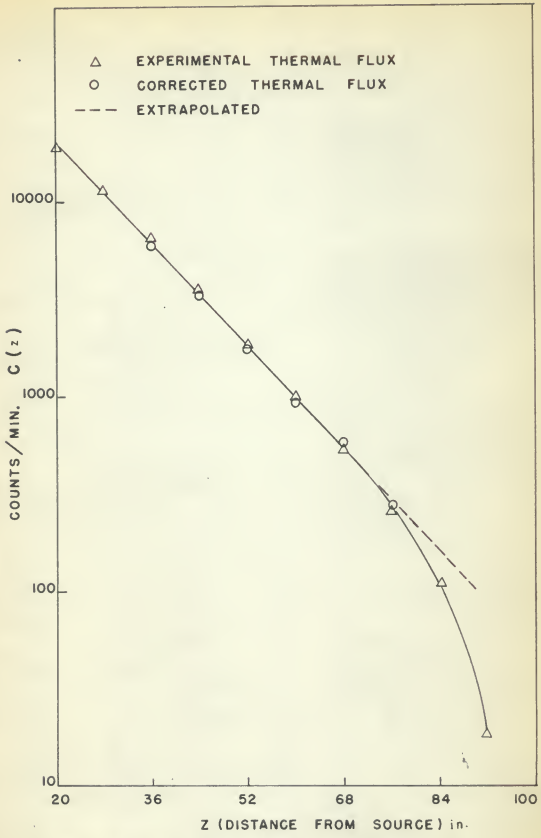

Fig. 24. Experimental data for determination of diffusion length.

thorough experimental investigation on the same graphite assembly using small BF_3 Nuclear Chicago counters and indium foils.

An L value much closer to the figure reported by Kaiser (15) could have been obtained had more data been taken. Since the purpose of the experiment was only to demonstrate the quality of the counter, no further attempts were made.

CONCLUSIONS

The following conclusions are drawn from the results of the present investigation.

1. It is possible to build up boron trifluoride counters with good characteristics using a relatively inexpensive vacuum system.

2. Counters should be cleaned very thoroughly before being sealed onto the vacuum system and should then be heated to about 250° C for 12 hours, then to 400° C for two hours while maintaining the pressure below 10^{-4} mm Hg to drive off occluded gases.

3. Glass stopcocks and stopcock grease in particular should be completely avoided in vacuum systems used for filling BF_3 counters.

4. Experimental sensitivity of the counter prepared was much less than its theoretically calculated sensitivity, probably due to the eccentricities in anode wires, incomplete cleaning of counter, and/or inaccurate evaluation of the counter sensitive volume.

5. Efficiency of the prepared counter for gamma rays was of the order of 10^{-4} of its efficiency for neutrons. Increase in amplifier gain raised the counter efficiency for gammas but was always below 5×10^{-4} of the efficiency for neutrons.

6. Determination of diffusion lengths of thermal neutrons in graphite using the prepared counter yielded, based on the one set of data obtained, a value reasonably close to that determined by indium-foils irradiation technique. Better values could have been achieved by improving counting statistics and by taking the depression in neutron flux caused by the presence of this relatively large counter in consideration.

ACKNOWLEDGMENT

Appreciation is expressed to Dr. S. Z. Mikhail, major instructor, for his valuable guidance and counsel through the entire research, coupled with his encouragement throughout the course of this investigation and the preparation of this manuscript.

The author would also like to make grateful acknowledgment to Dr. William R. Kimel, Head of the Department of Nuclear Engineering, for his initiating and supporting this research.

In addition, appreciation is extended to the staff and students of the Department of Nuclear Engineering for their helpful suggestions.

LITERATURE CITED

1. Alpert, D. and R. S. Buritz.
Ultra-high vacuum. II. Limiting factors on the attainment of very low pressures. J. of Appl. Physics. 25:202. 1954.

2. Alpert, D.
New developments in the production and measurement of ultra-high vacuum. J. of Appl Phys. 24:860. 1953.

3. Alpert, D.
Experiment at very low pressure. Science. 122:729. 1955.

4. Aponte, J. D., and S. A. Korff.
Effect of gaseous impurities on BF_3 proportional counter. Rev. of Sci. Inst. 31:532. 1960.

5. Bistiline, J. A.
Some properties of BF_3 in ionization chambers. Rev.of Sci. Inst. 19:842. 1948.

6. Booth, H. S., and D. R. Martin.
Boron trifluoride and its derivatives. New York: John Wiley & Sons, Inc., 1949.

7. Bradbury, N. E.
Formation of negative ions in gases by electron attachment. J. Chem. Phys. 2:827. 1934.

8. Brower, S., L. Bretcher, and Yilhent.
Proc. Cambridge Phil. Soc. 34:290. 1938.

9. Ferguson, G. A., and F. E. Jablonski.
Electron mobility in boron trimethyl. Rev. of Sci. Inst. 28:893. 1957.

10. Fowler, I. L., and P. P. Tuncliffe.
Boron trifluoride proportional counters. Rev. Sci. Inst. 21:737. 1950.

11. Glasstone, S., and M. C. Edlund.
The elements of nuclear reactor theory. New York: D. Van Nostrand Company, 1958.

12. Foulke, L.
M. S. thesis, Kansas State University, Manhattan, Kansas, 1961.

13. Hickman, W. M., and R. E. Fox.
Electron attachment in sulphur hexafluoride using monoenergetic electrons. J. Chem. Phys. 25:642. 1956.

14. Hudswell, F., S. Nairn, and Willkinson.
Boron trifluoride for neutron detection. A.E.R.E., C/R651. Harwell, Berkshire, England. 1951.

15. Kaiser, R.
Unpublished thesis, Kansas State University, 1961.

16. Korff, S. A.
Electrons and nuclear counters. New York: D. Van Nostrand Company, Inc., 1946.

17. Lloyd, S., W. Hodges, and A. Weinstock.
Preparation of boron trifluoride for use in neutron counters. A.E.C.D. 2223.

18. Petree, G., C. H. Johnson, and D. W. Miller.
Detection of boron by fast neutrons. Phys. Rev. 83:1148. 1951.

19. Price, W. J.
Nuclear radiation detection. New York: McGraw-Hill Book Company, Inc., 1958.

20. Rose, M. E., and S. A. Korff.
Properties of proportional counters. Phys. Rev. 59:850. 1941.

21. Rossi, B. B., and H. H. Staub.
Ionization chambers and counters. New York: McGraw-Hill Book Company, Inc., 1949.

22. Wilkinson, D. H.
Ionization chambers and counters. Cambridge: Cambridge University Press, 1950.

APPENDIX

APPENDIX[1]

Determination of Gas Multiplication Factor

The expression for the multiplication factor in terms of the counter parameters has been deduced by Rose and Korff (20). The equation for the gas multiplication was obtained under the following assumptions.

1. Secondary electron emission by positive ions at the cathode is negligible.

2. Recombination and electron attachment to neutral molecules are negligible. The recombination process is unimportant under high fields and in low pressure counters. Electron attachment for some gases is quite appreciable (16).

3. Photoelectric effect at the cathode is negligible. For polyatomic molecules this assumption holds fairly well.

4. The fluctuation in avalanche process can be neglected. Considering that a single electron arriving from the initial ionization produces further electrons, and denoting the number of such electrons at a distance r from the center wire by N(r), the integral equation for the increase of N(r) when r decreases by dr can be written as (20):

$$-dN = N(r)\, dr \int_0^{\epsilon_{max}} \frac{n(\epsilon, r)}{1(\epsilon)}\, d\epsilon \qquad (1)$$

---

[1]Quoted from Rose, M. E. and S. A. Korff. Phys. Rev. 59: 850. 1941.

Here ϵ denotes the excess of the electron energy over the (average) ionization potential of the gas in the counter. For the sake of brevity, the excess energy ϵ is referred to as "the energy". In equation (1) $n(\epsilon, r)d\epsilon$ is the fraction of electrons at r with energy between ϵ and $\epsilon + d\epsilon$, that is, the energy distribution normalized to unity. $l(\epsilon)$ is the mean free path for the ionization and ϵ max is the maximum energy of the electron at r. The integral in (1) is thus simply the average number of ionizing collisions per unit distance and is denoted by K(r), so that from equation (1)

$$N(r) = \exp \int_{r}^{r_o} K(r)\, dr \qquad (2)$$

In equation (2), r_o is introduced as the distance from the center of the wire at which the avalanche-producing-ionization starts.

The amplification factor A is then given by $N(r_1)$ where r_1 is the radius of the wire,

$$A = N(r_1) = \exp \int_{r_1}^{r_o} K(r)\, dr \qquad (3)$$

It is seen, as may have been anticipated, that the main task of the theory is the calculation of the average number of ionizing collisions per unit distance, K(r), and the spatial extent of the ionization region r_o. Considering the former quantity, it is clear that in principle a knowledge of the energy distribution at each point r is involved, although all that is eventually required is the average value of a known function of the energy, viz:

$$K(r) = \left[1/\ell(\epsilon)\right]_{AV} \qquad (4)$$

In order to specify the energy dependence of the mean free path, it should be recognized that the electrons attain an energy of the order of the ionization potential ($\backsim$15 volt) at a point very near the wire and that the energy gain in the region of ionization is sufficiently slow so that the electron energy at the wire is only a few times the ionization potential. The energy region pertinent to our consideration is such that the ionization cross section increases linearly with energy. Hence writing for the cross section

$$\sigma(E) = a\epsilon \tag{5}$$

where a is a constant depending on the nature of the gas, and for the mean free path

$$\ell(\epsilon) = 1/aN_m\epsilon \tag{5a}$$

where N_m is the number of molecules per unit volume, equation (4) takes the form,

$$K(r) = aN_m\epsilon_{AV} \tag{6}$$

In order to obtain the average energy ϵ_{AV}, the manner in which the energy distribution arises should be considered. The distribution, according to the present scheme (no fluctuations), arises from the fact that the electrons at r have different points of origin r' and the energy at r is given by the average energy gain in traversing the distances from r' to r. The average energy gain is determined by

$$-\frac{d\epsilon}{dr} = (C\ V_o/r) - \gamma(\epsilon) \tag{7}$$

Equation (7) determines ϵ for those electrons at r which have started from r', as a function of r and r' subject to the

initial condition

$$\epsilon(r = r') = 0$$

Here $\gamma(\epsilon)$ is the energy loss per unit distance due to all energetically possible inelastic processes, V_o is the voltage across the counter, and $1/C = \log(r_2/r_1)$ so that $\frac{1}{2}C$ is the capacity per unit length of the counter with r_2 the cylinder (cathode) radius.

According to the above, the number of electrons at r having an energy between ϵ and $\epsilon + d\epsilon$ is just the number which was formed at a distance between r' and r' + dr', where $dr' = (dr'/d\epsilon)d\epsilon$ and r' is given in terms of ϵ and r by equation (7). Thus the energy distribution at r depends on the distribution at r', and is accordingly given by the following integral equation:

$$N(r)\, n(\epsilon, r)d\epsilon = dr'\, N(r') \int_0^{\epsilon'_{max}} \frac{n(\epsilon', r')}{\ell(\epsilon')}\, d\epsilon \qquad (8)$$

where ϵ'_{max} is the maximum energy at r' and the actual number of electrons with energy between ϵ and $\epsilon + d\epsilon$, namely, $N(r')n(\epsilon', r')d\epsilon$ has been introduced.

An exact solution of this integral equation, and the determination of the distribution function itself, appears to be out of question, but the average energy may be obtained by the following approximate method.

It can be seen that $n(\epsilon, r)$ has the dimensions of $(\text{energy})^{-1}$, and hence can be written as

$$n(\epsilon, r) = \left(\frac{1}{\epsilon_{AV}}\right)\phi(\epsilon/\epsilon_{AV}) \qquad (9)$$

where ϕ is a dimensionless function of the indicated dimensionless argument and the dependence on r is contained in $\epsilon_{AV}(r)$. The essential approximation consists in the fulfillment of the integral equation only for those energies for which the number of electrons is greatest. Since more than half of the electrons at r were formed in the last mean free path, and since the more remote the point of origin (i.e., the greater the energy), the energy distribution will be monotonically decreasing with the most important energy region at $\epsilon = 0$. Thus by setting $r' = r$, $\epsilon = 0$,

$$\frac{d\epsilon}{dr'} = -\frac{d\epsilon}{dr} = \frac{c\ V_o}{r}$$

The average energy can be obtained at once from equation (8) with the help of equations (6) and (9):

$$\epsilon_{AV}(r) = \left(\frac{\phi(0)\ cV_o}{aN_m\ r}\right)^{\frac{1}{2}} \tag{10}$$

From the above equation we see that the average energy, and the width of the energy distribution which will be proportional to ϵ_{AV}, both increase as the electrons approach the wire, as was to be expected. From equation (6) the average number of ionizing collisions per unit distance follows immediately

$$K(r) = (\phi(0)\ aN_m\ c\ V_o/r)^{\frac{1}{2}} \tag{11}$$

The final step in the calculation is the consideration of r_o. According to the way in which this quantity was introduced in equation (2), it is the distance from the wire to the point at which the avalanche starts, and at this point one may expect fluctuations to play a more important role. Calculation of this

constant in terms of the physical constants will give an expression for multiplication.

According to equation (10), introducing a factor ϵ_o, which is defined as the "critical energy", and is the average energy at the point where the ionization starts, can be written as

$$\epsilon_o = \left(\frac{\phi(0)}{a N_m} \quad \frac{(C V_o)}{r_o} \right) \tag{12}$$

The critical energy ϵ_o will depend on the nature of the gas (ionization potential and cross section) but will not depend on the counter voltage or geometrical factors. It follows from equation (12) that r_o increases linearly with the counter voltage for which ionization does not begin until the electron reaches the wire, i.e., $r_o = r_1$. At this voltage for the proportional region, the multiplication factor becomes unity and below this voltage the counter acts as an ionization chamber.

Denoting the proportional threshold by V_p, the expression for r_o can be written as

$$r_o = r_1 \, V_o/V_p \tag{13}$$

With equations (13) and (11), the expression for multiplication can be written as

$$A = \exp 2(aN_m \, C \, r_1 \, \phi(0) \, V_o)^{\frac{1}{2}} \left[(V_o/V_p)^{\frac{1}{2}} - 1 \right] \tag{14}$$

in which, as mentioned above, $\phi(0)$ is to be set equal to unity[1] and V_p is to be determined from the measurements. The quantity a in equation (14) is the rate of change of the ionization cross section for energies just above the ionization potential.

---

[1]The quantity $\phi(0)$ which occurs in these results and which is essentially the number of slowest electrons, cannot be evaluated uniquely without knowing the actual form of the distribution function. However, the function ϕ is sufficiently restricted so that $\phi(0)$ cannot, in general, vary over wide limits. In addition to the requirement that ϕ shall be a monotonically decreasing function of its argument, there are two further conditions to be imposed on this function. With $x = \epsilon/\epsilon_{AV}$, the normalization condition is

$$\int_0^\infty \phi(x)\, dx = 1$$

and from the definition of x,

$$\int_0^\infty x\, \phi(x)\, dx = 1$$

Various functional forms for ϕ may be assumed and after the first condition has been imposed, ϕ may be calculated.

CONSTRUCTION AND CHARACTERISTICS OF BF_3 TUBES USED IN DETERMINATION OF REACTOR PARAMETERS

by

MOHAMMED NASIM

B. Sc., Karachi University, 1952
M. S., Government College, Punjab University, 1954

AN ABSTRACT OF
A MASTER'S THESIS

submitted in partial fulfillment of the

requirements for the degree

MASTER OF SCIENCE

Department of Nuclear Engineering

KANSAS STATE UNIVERSITY
Manhattan, Kansas

1961

A glass vacuum system was constructed for purification of boron trifluoride gas and filling of the BF_3 counters. Pressures of the order of 10^{-5} mm Hg were achieved and could be maintained for intervals of 24 hours by this system.

Two different counters (A) and (B) were constructed, cleaned thoroughly, sealed to the vacuum system, outgassed at 250° C for 12 hours and at 400° C for two hours, with the pressure maintained below 10^{-4} mm Hg. The counters were filled with BF_3 gas at 32.0 and 29.9 cm pressures, respectively. Details of construction of the counters and the effect of impurities in BF_3 gas on the counter performance are discussed.

Boron trifluoride gas was prepared by thermal dissociation of 96 per cent B^{10} enriched BF_3CaF_2 and purified by repeated condensation at liquid air temperatures. Purity of the gas was checked by measuring its boiling point, using a Cu-Constantan thermocouple. Typical plots of the time-temperature variation of the boiling BF_3 are given.

Variations of gas multiplication of counter (B) with changes in the voltage applied to the counter were studied. Experimental values of multiplication were compared with their corresponding theoretical values calculated from equations derived by Rose and Korff (20). Discrepancies between the theoretical and experimental values at lower voltages were attributed to the asymptotic nature of the Rose and Korff equation.

Sensitivity of counter (B) for thermal neutrons was determined by inserting it in several positions in the Kansas State University graphite subcritical reactor which has been

standardized so that the neutron flux is known throughout the assembly. Dependence of the counter sensitivity on the distance between the counter and the source was studied. Sensitivity was found to increase with the increase in distance up to about 1.5 diffusion lengths where it remained constant. This was attributed to the fact that at smaller distances, neutrons are not adequately slowed down and the cross section of B^{10} (n, α) reaction is correspondingly lower. Experimental values of sensitivity were always much less than the theoretical sensitivity calculated by the formula given by Price (19). Discrepancy was attributed to eccentricities in anode wire, incomplete cleaning of the counter and/or inaccurate evaluation of the counter sensitive volume.

A number of plateau curves were obtained for different amplifier gain settings. The best plateau was obtained at a gain of 8. Increase of amplifier gain decreased the horizontal part of the plateau.

An integral bias curve was obtained applying 1475 volts to the counter. The relatively broad distribution in the number of counts was attributed to the partial ionization loss of the disintegration products which strike the wall of the counter.

The efficiency of the counter to gamma rays relative to its efficiency to neutrons was determined at different amplifier gain settings. This relative efficiency was found to increase with increase of amplifier gain but not to exceed 5×10^{-4}.

The diffusion length of neutrons in graphite was determined in the Kansas State University graphite subcritical assembly

using counter (B). Based on one set of data, a value of 57.32 cm was obtained. A better value could have been obtained by improving the statistics of counting, by repeating the experiment, and by allowing for the flux depression due to the presence of this relatively large counter. Since the purpose of the experiment was only to demonstrate the quality of the counter, no further attempts were made to measure diffusion length.